FINAL TECHNICAL REPORT

MAP OF ACTIVE FAULT TRACES, GEOMORPHIC FEATURES AND QUATERNARY SURFICIAL DEPOSITS ALONG THE CENTRAL CALAVERAS FAULT, SANTA CLARA COUNTY, CALIFORNIA

Recipient:

William Lettis & Associates, Inc.
1777 Botelho Drive, Suite 262
Walnut Creek, CA 94596
Phone: (925) 256-6070; Fax: (925) 256-6076

Principal Investigators:

Robert C. Witter[1], Keith I Kelson[1], Andrew D. Barron[1,2], and Sean T. Sundermann[1]

[1]William Lettis & Associates, Inc.
1777 Botelho Drive, Suite 262
Walnut Creek, CA 94596
Phone: (925) 256-6070; Fax: (925) 256-6076
E-mail: witter@lettis.com

[2]Current address:
Center for Neotectonic Studies MS 169
University of Nevada, Reno
Reno, NV 89557

Program Element II
Keywords: Paleoseismology, Geologic Mapping, Surficial Deposits, Tectonic Structures

U.S. Geological Survey
National Earthquake Hazards Reduction Program
Award No. 01HQGR0212

July 2003

Research supported by U.S. Geological Survey (USGS), Department of Interior, under USGS award number 01HQGR0125. The views and conclusions contained in this document are those of the authors and should not be interpreted as necessarily representing the official policies, either expressed or implied, of the U.S. Government.

TABLE OF CONTENTS

LIST OF TABLES

LIST OF FIGURES

LIST OF APPENDICES

LIST OF PLATES

Award No. 01HQGR0212

MAP OF ACTIVE FAULT TRACES, GEOMORPHIC FEATURES AND QUATERNARY SURFICIAL DEPOSITS ALONG THE CENTRAL CALAVERAS FAULT, SANTA CLARA COUNTY, CALIFORNIA

Robert C. Witter[1], Keith I Kelson[1], Andrew D. Barron[1,2], and Sean T. Sundermann[1]

[1]William Lettis & Associates, Inc.
1777 Botelho Drive, Suite 262
Walnut Creek, CA 94596
Phone: (925) 256-6070; Fax: (925) 256-6076

[2]Current address:
Center for Neotectonic Studies MS 169
University of Nevada, Reno
Reno, NV 89557

E-mail: witter@lettis.com

ABSTRACT

The central Calaveras Fault accommodates nearly fifty percent of Pacific-North American plate motion in the San Francisco Bay area. Historical creep data and geodetic studies estimate the present rate of fault slip at 16 mm/yr. Trenching studies suggest a 14 ± 5 mm/yr late Holocene geologic slip rate at the latitude of Gilroy. Historical moderate earthquakes (M 5 to 6) have occurred on the central Calaveras Fault, but no conclusive evidence for surface fault rupture caused by these events has been reported.

This map depicts surficial fault traces active in the Holocene (<11,000 years old) along the central section of the Calaveras Fault between Calaveras Reservoir in the north to San Felipe Lake in the south. Five sources of data were used to map active fault traces: (1) geomorphic expression; (2) earthquake-related ground deformation; (3) evidence for aseismic slip (historic creep); (4) previous geomorphic and geological mapping; and (5) limited published and unpublished geological reports. The map and source data are compiled in a digital database at the scale of 1:24,000 and cover parts of nine 7.5-minute quadrangles including, Calaveras Reservoir, San Jose East, Mt. Day, Lick Observatory, Morgan Hill, Mount Sizer, Gilroy, Gilroy Hot Springs and San Felipe.

Patterns in the surficial expression of the fault traces identified on this map appear to reflect seismogenic subsegments of the central Calaveras Fault. The surface projection of microseismicity, including aftershocks of the 1949, 1979, 1984, and 1988 earthquakes, does not coincide with the mapped trace of the fault at the surface. However, geometric characteristics of the surface fault trace, including releasing bends and stopovers, correlate with historical earthquake rupture geologic slip rate estimates lengths and may reflect subsurface rupture barriers along the fault. Considering the lack of conclusive evidence for surface fault rupture during historical M >5 earthquakes, and historic creep rates that approach the geologic slip rate estimates, patterns of surficial fault traces depicted on this map suggest that earthquakes on the central Calaveras Fault historically have involved to 2.5- to 26-km-long subsegments. However, these observations do not preclude the possibility that future earthquakes may break multiple subsegments of the fault.

1.0 INTRODUCTION

Probabilistic seismic hazard estimates for the San Francisco Bay region forecast an 18-percent chance for a large-magnitude (M ≥6.7) earthquake on the Calaveras Fault by the year 2030 (WGCEP, 1999). Yet considerable uncertainty exists regarding whether the Calaveras Fault is capable of producing large earthquakes or predominantly releases elastic strain through moderate-magnitude (M 5.1 to 6.2) earthquakes and aseismic slip (creep). Further uncertainty arises from the ambiguity of fault segmentation models used to estimate rupture length and earthquake recurrence times. The fault strip map presented in this report (Figure 1; Plates 1 and 2) focuses on the central Calaveras Fault, a 64-km-long, actively creeping section of the fault that is well characterized by microseismicity and moderate earthquakes but lacks a well documented paleoseismic record. The physical characteristics of the active fault traces illustrated by this map provide new data to evaluate earthquake source parameters for the Calaveras Fault that are necessary to improve estimates of probabilistic ground motions for the rapidly expanding San Jose and Santa Clara urban centers.

The primary purpose of this map is to evaluate segmentation models and the seismic potential of the central Calaveras Fault by characterizing the surficial expression and geometry of active fault traces. Detailed mapping of active fault traces contributes information on the lateral continuity, relative complexity and kinematics of the fault zone. Such surficial characteristics provide physical constraints to better estimate the length of possible surface-fault rupture, the amount of possible coseismic surface displacement, the style of surface deformation due to aseismic fault creep, and likely recurrence intervals of moderate- to large-magnitude earthquakes. A secondary objective of the project is to assess fault activity by mapping Quaternary surficial deposits adjacent to and displaced by the fault. The map delineates recently active fault traces that potentially cut late Holocene deposits and can be used to identify sites for future paleoseismic study to better estimate geologic slip rates, the amount of coseismic or aseismic slip and, if present, prehistoric earthquake chronologies.

This map shows the location of active (Holocene) traces of the central Calaveras Fault and Quaternary surficial deposits adjacent to and cut by the fault (Plates 1and 2). An active fault trace, as defined in this study, is a fault that displaces Holocene deposits younger than 11,000 years old. Five sources of data were evaluated to map active fault traces: (1) geomorphic expression; (2) earthquake-related ground deformation; (3) evidence for aseismic slip (historic creep); (4) previous geomorphic and geological mapping; and (5) limited published and unpublished geological reports. The data are compiled in a digital database at the scale of 1:24,000 that covers parts of nine 7.5-minute quadrangles including, Calaveras Reservoir, San Jose East, Mt. Day, Lick Observatory, Morgan Hill, Mount Sizer, Gilroy, Gilroy Hot Springs and San Felipe (Figure 1). Based on the complex architecture of active surficial traces and the distributed nature of surface deformation depicted on the map, the central Calaveras Fault is a multi-segmented fault zone that partitions slip from the San Andreas Fault south of Hollister onto the southern Hayward and northern Calaveras Faults near Calaveras Reservoir. This slip appears to be accommodated along the southern and central Calaveras Faults by aseismic creep and moderate magnitude earthquakes.

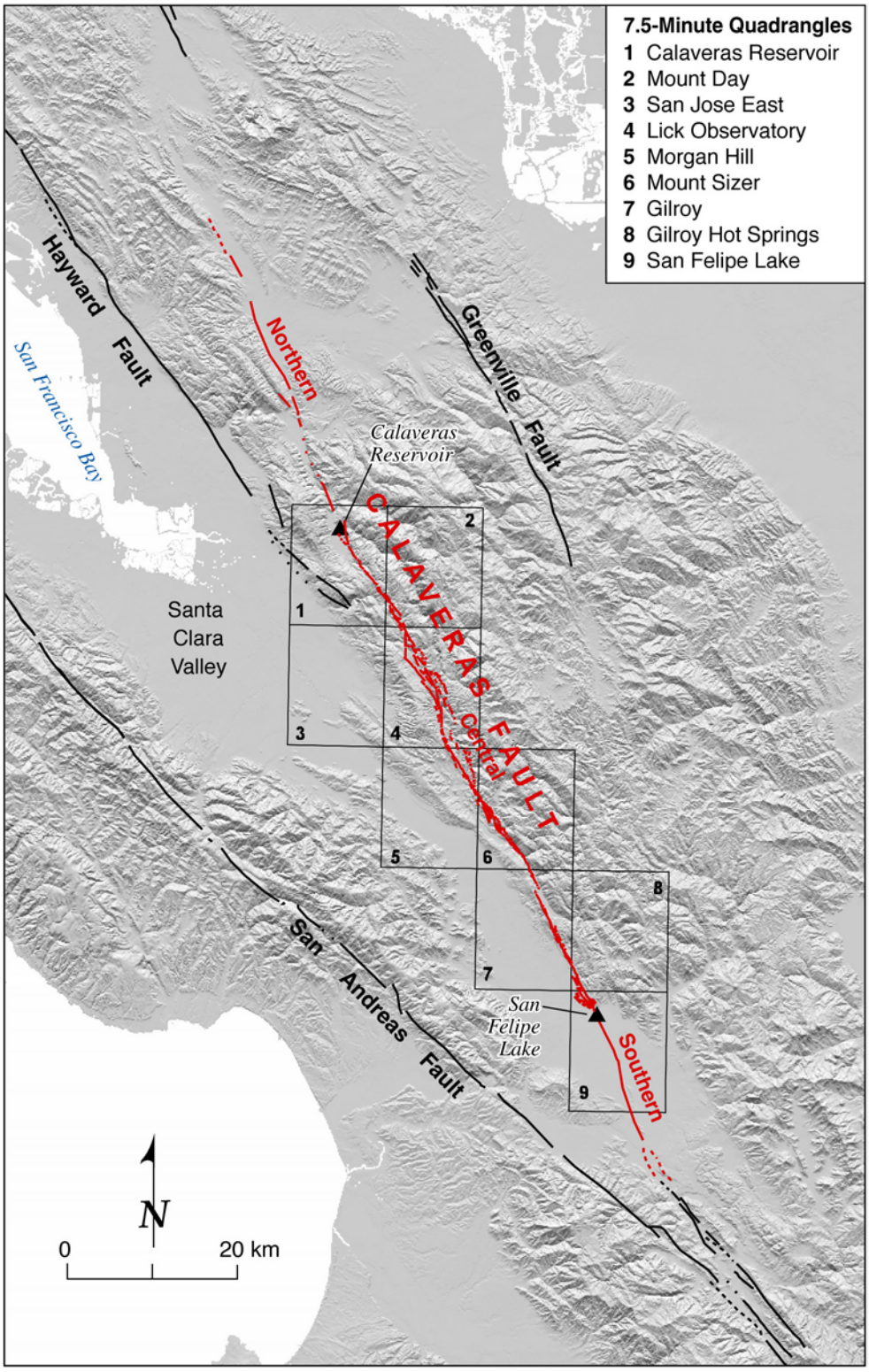

Figure 1. Shaded relief map of southern San Francisco Bay region, showing the Calaveras fault and its major segments (shown by ▲'s). Map area along the central Calaveras fault includes parts of nine quadrangles shown with boxes. Surficial deposits on Calaveras Reservoir and San Jose East quadrangles have been mapped at 1:24,000.

1.1 Geologic and Seismotectonic Setting

The 142-km-long Calaveras Fault zone is an active right-lateral transform fault that accommodates 24- to 35-percent of the relative motion between the Pacific and North America plates at the latitude of the southern San Francisco Bay area (Figure 1). A relatively young structure compared to the San Andreas Fault, the Calaveras Fault zone originated in the Pliocene and has laterally displaced Miocene sediments and Plio-Pleistocene folds by 16 to 24 km since 2.8 to 3.6 Ma (Page, 1982). The 0.1- to 2-km-wide fault zone consists of braided and en echelon fault traces, sub-parallel linear fault strands, left-restraining double bends and right-releasing stepovers that have developed, in part, along pre-existing faults such as the Madrone Springs Fault (Figure 2). The strikes of the various active traces differ by as much as 33° and together define a regional strike of about N 26° W within the transpressional seismotectonic domain of the southeastern San Francisco Bay region (Aydin, 1982; Unruh and Lettis, 1998). Cross-sections of precisely located seismicity within the Calaveras Fault zone resolve a subvertical fault plane that in some areas dips about 85° to the east, exhibits a 1-km-wide left restraining stepover, and extends to the base of the seismogenic zone at ~9 km (Schaff et al., 2002). Between San Felipe Valley and Anderson Lake, seismicity data shows a ~30° northeast-dipping blind thrust fault that strikes parallel to and appears to join the Calaveras Fault at depth (Schaff et al., 2002).

Kelson et al. (1998) identified three sections of the fault zone that are distinct from one another based on contemporary seismicity, structural relations with adjacent faults, present-day creep rates, and geomorphic expression. These sections, which may or may not reflect earthquake rupture segments, include, (1) the northern Calaveras Fault extending from Danville to Calaveras Reservoir; (2) the central Calaveras Fault extending from Calaveras Reservoir to San Felipe Lake; and (3) the southern Calaveras Fault extending from San Felipe Lake to the Paicines Fault, south of Hollister (Figure 1). The central and southern sections of the Calaveras Fault zone inherit 17 ± 4 mm/yr of dextral slip (Kelson, 2001; Kelson et al., 1998; Lienkaemper et al., 1991) partitioned from the San Andreas Fault that accommodates about 34 mm/yr of Pacific-North America plate motion south of latitude 36.5° N (Sieh and Jahns, 1984). To the north, the central Calaveras Fault partitions slip at a rate of 8 to 10 mm/yr onto the southern Hayward Fault (Lienkaemper et al., 1991) and 4 to 7 mm/yr onto the northern Calaveras Fault (Kelson et al., 1992; 1996; Simpson et al., 1999). Along the central Calaveras Fault at San Ysidro Creek near Gilroy paleoseismic investigations provide a late Holocene slip rate estimate of 8 to 19 mm/yr (Baldwin et al., 2002). Controversial evidence for coseismic rupture at this site suggests that three earthquakes occurred between 4,100 to 2,500 years ago with 2- to 2.5-m of right-lateral displacement per event (Kelson et al., 1998). Near Coyote Lake, an alignment array installed by the U.S. Geological Survey in 1968 yields an historic creep rate estimate of 13 to 14 mm/yr from 1968 to 1999 (J. Galehouse and J. Lienkaemper, written comm., 1999).

The central Calaveras Fault traverses obliquely through steep topography of the Diablo Range composed chiefly of Coast Range ophiolite and Franciscan rocks overlain by right-laterally displaced and uplifted Neogene sediments (Page, 1982). Northwest of San Felipe Valley and east of the fault, rocks of the Eastern Belt Franciscan Complex are placed against Cretaceous sediments of the Berryessa Formation and Tertiary deposits to the west (Page, 1982; Wentworth

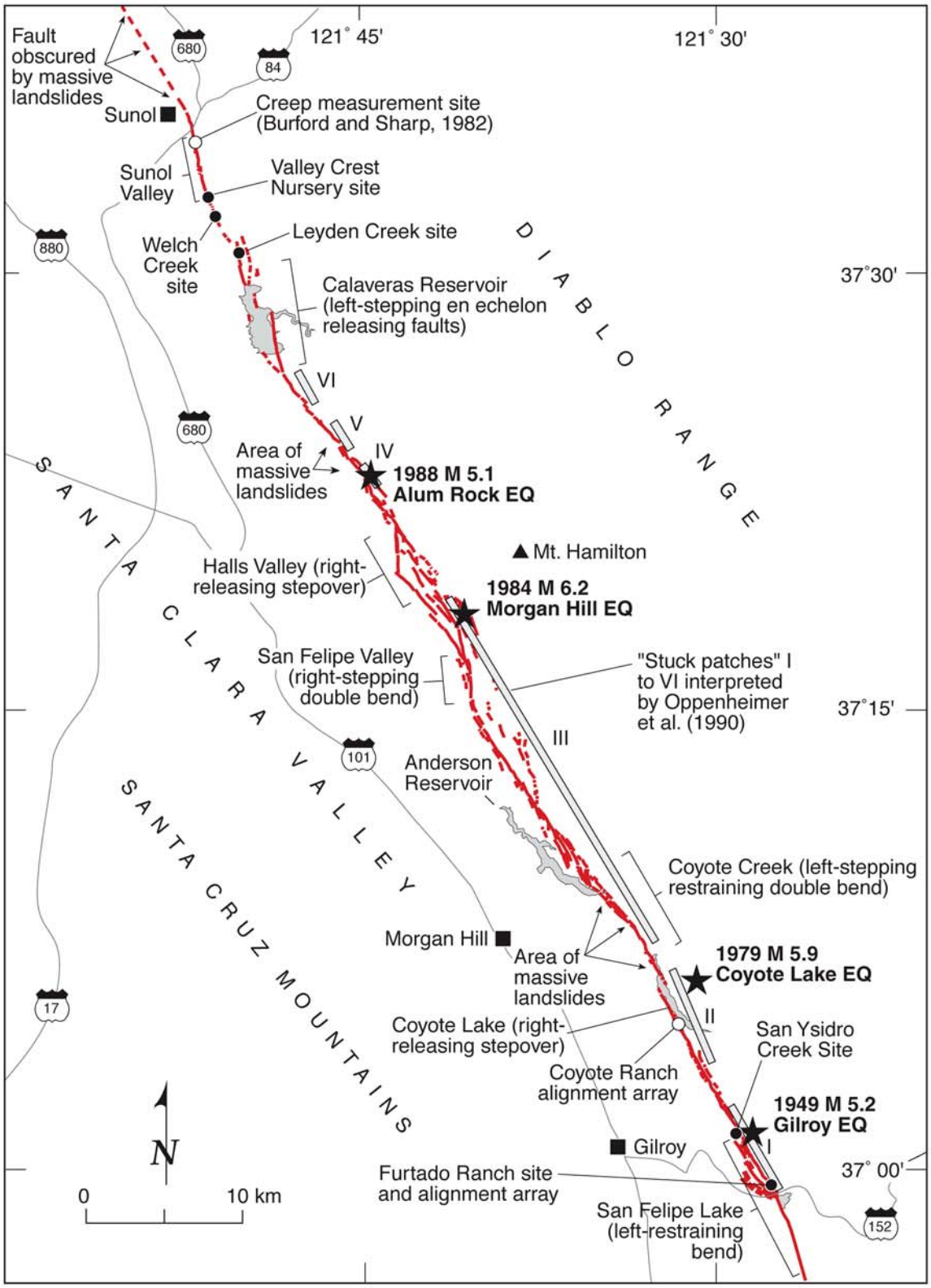

Figure 2. Simplified map of the central Calaveras fault, showing paleoseismic sites, existing creep measurement sites and distinct kinematic elements based on fault geometry. Historic M >5 earthquakes (stars) and "stuck patches" (bars labeled I to VI) from Oppenheimer et al. (1990).

et al., 1999). Southeast of San Felipe Valley, predominantly Cretaceous marine deposits east of the fault are juxtaposed against Tertiary volcanic and sedimentary rocks and Plio-Pleistocene nonmarine deposits including the Silvercreek and Packwood gravels to the west (Wentworth et al., 1999). Southwest of the fault, steep east-dipping right-lateral, oblique-reverse and low-angle west vergent thrust faults, including the Silvercreek, Evergreen and Quimby Faults, accommodate transpressional deformation as slip steps right from the central Calaveras Fault to the southern Hayward Fault (Wentworth et al., 1999). Uplift of rocks in the Diablo Range at rates of 1.4 to 2 mm/yr since 3.5 Ma principally have been accommodated by thrust faulting and folding that only passively involved the Calaveras Fault (Page et al., 1998).

Abundant microseismicity and several historic moderate-magnitude earthquakes (Table 1) characterize the central Calaveras Fault (Figure 3) (Bakun, 1980; Bakun et al., 1984; Bakun and Lindh, 1985; Cockerham and Eaton, 1987; Oppenheimer et al., 1990; Schaff et al., 2002). Three consecutive M >5 earthquakes ruptured the fault in a northward progression as post-seismic relaxation following one event triggered the next event (Du and Aydin, 1992). The series began with the 1979 M 7.9 Coyote Lake earthquake, succeeded by the 1984 M 6.2 Morgan Hill earthquake, and ended with the 1988 M 5.1 Alum Rock earthquake (Oppenheimer et al., 1990). The Coyote Lake and Morgan Hill rupture areas appear to have slipped previously in 1897 and 1911, respectively (Oppenheimer et al., 1990; Toppozada and Parke, 1982; Toppozada et al., 1981). Through the analysis of spatial patterns of microseismicity before and after historic earthquakes, Oppenheimer et al., (1990) identified six aseismic regions of the fault that appear to be locked (Figure 2). Two of the regions ("patches" II and III) coincide with areas of high slip distribution during the Coyote Lake and Morgan Hill earthquakes. Two other regions, one near Gilroy ("patch" I) and a second located south of Calaveras Reservoir ("patch" IV), are the most probable sites for the next M >5 earthquake (Figure 2) (Oppenheimer et al., 1990).

Table 1. Historical seismicity greater than M 5.0 along the central Calaveras fault

Date	Mag	Latitude	Longitude	Depth	Name	Reference
20 Jun 1897	6.2	37°N 00'	121°W 30'	--	--	Toppozada et al., 1981
6 Jul 1899	5.8	37°N 12'	121°W 30'	--	--	Toppozada et al., 1981
1 Jul 1911	6.5	37°N 18.5'	121°W40.7'	~8.5	Morgan Hill	Oppenheimer et al., 1990
26 Oct 1943	5.1	37°N 23.22'	121°W44.59'	8.55	Alum Rock	Oppenheimer et al., 1990
9 Mar 1949	5.2	37°N 01.2'	121°W 28.8'	--	Gilroy	Bolt and Miller, 1975
5 Sep 1955	5.5	37°N 22.2'	121°W 46.8	--	--	Bolt and Miller, 1975
6 Aug 1979	5.9	37°N 06.24'	121°W 31.07'	8.95	Coyote Lake	Oppenheimer et al., 1990
24 Apr 1984	6.2	37°N 18.56'	121°W 40.68'	8.42	Morgan Hill	Oppenheimer et al., 1990
31 Mar 1986	5.7	37°N 28.17'	121°W 41.63'	8.54	Mt. Lewis	Oppenheimer et al., 1990
13 Jun 1988	5.1	37°N 23.22'	121°W 44.59'	8.55	Alum Rock	Oppenheimer et al., 1990

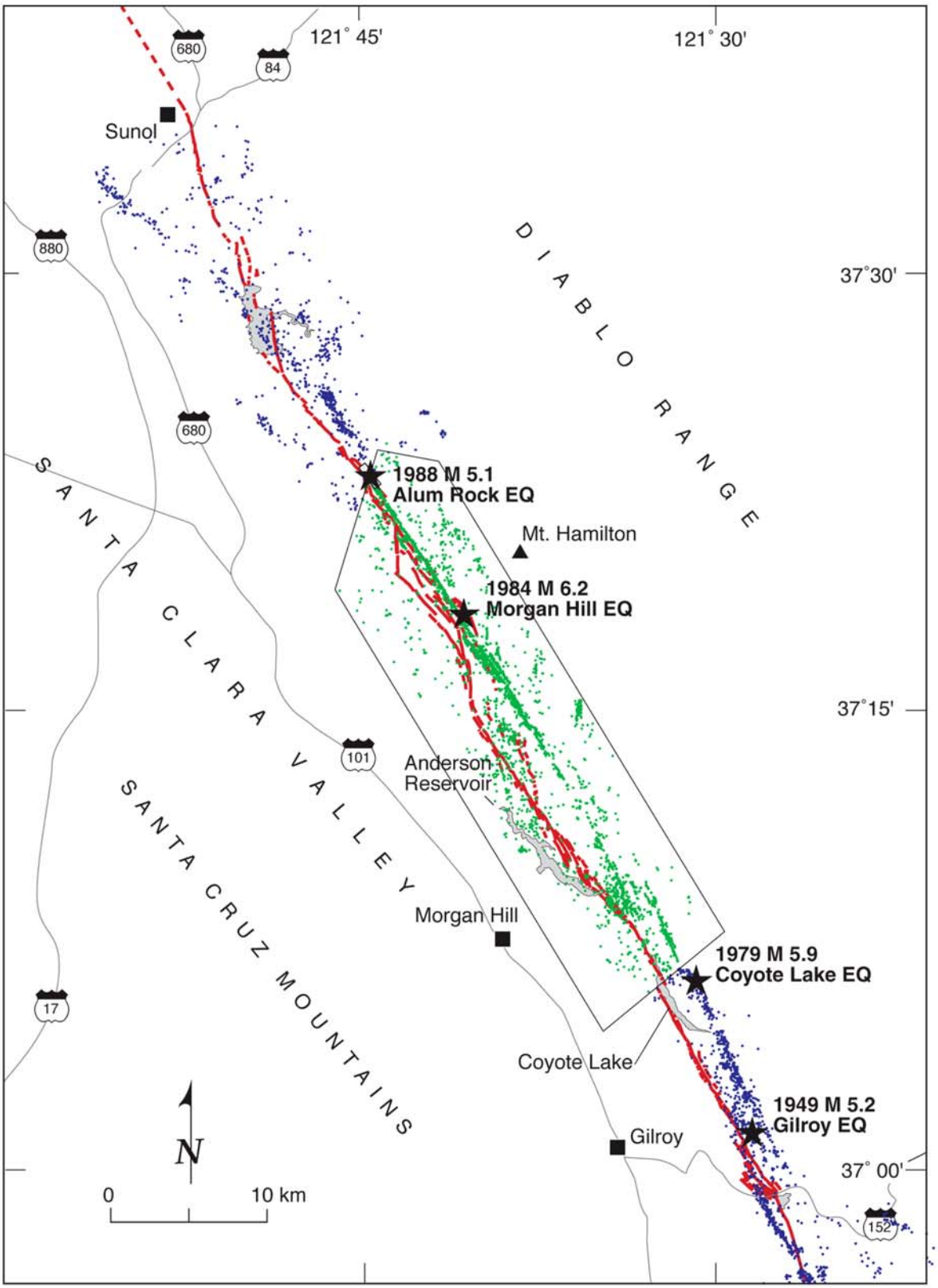

Figure 3. Historical seismicity (blue) from the Northern California Earthquake Data Center and relocated microseismicity (green) from Schaff et al. (2002) in bounding box. Historic M >5 earthquake epicenters (stars) from Oppenheimer et al. (1990).

1.2 Previous Mapping of the Central Calaveras Fault

Several existing geologic maps delineate the location of the central Calaveras Fault and provide a starting point from which we refine the location of fault traces and assess their activity. Some maps of the fault depict traces in bedrock, and do not directly assess the possibility of Holocene activity. Other fault maps show active traces based on geomorphic expression, evidence for active creep and interpretation of historic aerial photography, as summarized below.

Early maps by Crittenden (1951) depicted traces of the central Calaveras Fault east of San Jose in the Mt. Hamilton area. Regional mapping by Dibblee (1972a; 1972b; 1973a; 1973b; 1973c; 1973d; 1973e; 1975) featured prominent faults, including several traces of the Calaveras Fault, that offset Jurassic and Cretaceous bedrock and Tertiary deposits. Fault traces expressed in Franciscan rocks of the Diablo Range were mapped by Cotton (1972). Radbruch-Hall (1974) mapped "recently active breaks" indicative of Quaternary movement based on the evaluation of bedrock faults, geomorphic expression and limited creep data. Herd (unpublished mapping, cited in Bryant, 1981a) mapped Quaternary traces of the fault through the interpretation of 1939 aerial photography. Armstrong and Wagner (1978) and Wagner (1978) evaluated evidence for recent fault activity including historic creep for environmental geological surveys of the Diablo Range. Under mandate of the Alquist-Priolo Earthquake Fault Zoning Act of 1972 (Hart and Bryant, 1997), Bryant (1981a; 1981b; 1981c) and Smith (1981) evaluated active faults in central Santa Clara County and revised Special Studies Zones Maps through the interpretation of aerial photography, review of limited Alquist-Priolo reports and compilation of evidence for historic creep. Additional maps addressing the activity of the Calaveras Fault include work by Nakata (1980), Pampeyan, (1979), Rogers (1973) and Williams et al. (1973).

The map presented here (Plates 1 and 2) differs from earlier maps in that it depicts active traces of the central Calaveras Fault in the geologic context of Quaternary surficial deposits that lie adjacent to or are transected by or overlie the fault. The locations of the active fault traces and the distribution of associated Quaternary deposits are presented in a 1:24,000-scale digital database that includes detailed compilations of fault-related geomorphic features, sites of historic earthquake-related ground failure, evidence for historic creep, and limited geological data from published and unpublished reports. This map is not intended to replace the Earthquake Fault Zones Maps published by the California Geological Survey (Hart and Bryant, 1997) and does not provide sufficient information for site-specific development. Instead, this map compiles detailed geologic information related to fault activity and presents the data in a digitally accessible format for land use planners and geotechnical engineers interested in the mitigation of earthquake hazards. This map also provides a basis for interpreting the long-term behavior and segmentation of the Calaveras Fault, and thus, characterizes several seismic-source parameters useful for probabilistic and deterministic seismic hazard analyses.

2.0 APPROACH AND METHODS

Our approach includes the compilation of existing data on fault location and character of earthquake- or creep-related effects, analysis of vintage aerial photography to identify late Quaternary surficial deposits as well as fault-related geomorphic features, and the assembly of

these data sets to interpret patterns of Holocene displacement that characterize the central Calaveras Fault. The procedure used to map active fault traces and Quaternary surficial deposits follows that of Lienkaemper et al., (1991), applied to map active traces of the Hayward Fault, and Knudsen et al. (2000), developed to map Quaternary geologic units in the San Francisco Bay area. The map explanation (Appendix A) shows abbreviated symbols used to indicate specific geomorphic features, sites of historic creep, locations of earthquake-related surface deformation, and geologic study sites and associated reports. However, few trenching studies provide precise locations of Holocene or younger fault traces because the rugged terrain of the Diablo Range has not undergone significant urban development. Earliest available aerial photography (1939) provides a means to assess relatively undisturbed geomorphic conditions along the fault trace. Also, because of the relatively high relief along most of the central Calaveras Fault, high erosion rates may out pace the rate of tectonic-driven landscape change, and deep-seated landslides may sometimes obscure youthful geomorphic expression of faulting. Therefore, the active fault traces depicted on the map represent interpretations of multiple sources of data that individually may or may not directly indicate Holocene activity but together provide sufficient evidence to make a reasonable judgement regarding the likelihood of Holocene displacement.

2.1 Geomorphic Expression of Active Faults

Earthquake-related geomorphic features interpreted from aerial photography, topographic maps and field observations provide essential data to evaluate the activity of fault traces and develop 5- to 7-km-wide strip maps that characterize patterns of faulting over distances of tens to hundreds of kilometers (e.g., Lienkaemper, 1992; Sharp, 1972; Wallace, 1990). Active transform faults like the Hayward, San Andreas and Calaveras Faults produce recognizable landforms that appear at small scales (<1:250,000) as linear topographic discontinuities such as faceted mountain fronts, aligned linear valleys and chains of lakes and ponds (Wallace, 1990). At larger scales (>1:250,000), the geomorphic expression of active strike-slip faults often display complex patterns of strain common to many fault zones, including en echelon organization of fault traces, anastomosing secondary fault splays, extensional fault-bound basins formed by releasing stepovers, and antiformal pop-up structures formed by restraining stepovers (Barka and Kadinsky-Cade, 1988; Campagna and Aydin, 1991; Lettis et al., 2002).

At local scales (>1:24,000), distinct geomorphic features characterize active faults owing to both vertical and lateral displacement of surficial deposits and landforms (Wallace, 1990). The map (Plates 1 and 2) uses detailed geomorphic codes defined in the map explanation (Appendix A) to identify active traces of the central Calaveras Fault. The most reliable geomorphic features indicative of active traces include closed depressions and sag ponds (cd), graben (gr), offset or deflected stream channels (od, dd), scarps in young alluvium (sc), side-hill benches and troughs (sb, st), ponded or dammed alluvium (pa), and strongly pronounced tonal and vegetation lineaments (t, v). Other features, such as faceted and linear ridges (fr, lr), linear stream valleys and gullies (ls, lt), aligned notches and saddles (n, s), linear geologic contacts (gc), and shutter ridges (sr), provide equivocal evidence for active faulting because such features may reflect erosional processes or persist through time due to erosional enhancement or modification (Smith, 1981).

Following the methodology of Lienkaemper (1992), geomorphic features are ranked according to a scale of clarity by using the following codes: G1 indicates strongly pronounced features; G2 indicates distinct features; and G3 indicates features with weaker expression. Features of uncertain tectonic origin are queried. The geomorphic codes do not reflect the degree of confidence in the judgement that particular fault traces are of Holocene age. Instead, where evidence for Holocene displacement is less certain, the map delineates the fault trace as a dotted line or queried dotted line. This component of our methodology represents a departure from that of Lienkaemper (1992). The accuracy of active fault locations relates to the clarity of geomorphic expression as well as any additional lines of evidence that accurately delineate the fault. For example, sections of the fault characterized by strongly pronounced and distinct features (G1 or G2) that coincide with creep evidence and/or geological evidence for Holocene displacement can be more accurately located than ambiguous fault traces defined by weakly expressed features that lack evidence for creep or geologic information derived from paleoseismic trenches. Uncertainty in the location of fault traces is expressed by varying line types in the following way: (1) solid lines indicate well located traces (≤±25 m); (2) dashed lines indicate traces located with less certainty (≤±50 m); and (3) dotted lines indicate concealed or inferred fault traces (≤±75 m).

2.2 Ground Deformation Related to Historic M >5 Earthquakes

Abundant evidence for earthquake-induced ground failure occurred along the central Calaveras Fault during and shortly after historic M >5 earthquakes, including the 1897 event (Toppozada et al., 1981), the 1979 Coyote Lake event (Armstrong, 1979; Cotton et al., 1979; Hart et al., 1979), and the 1984 Morgan Hill event (Harms et al., 1984; Hart, 1984). Ground deformation codes compiled on the map indicate several types of earthquake-related effects, including cracks aligned with the mapped Quaternary fault trace (ac), accelerated post-seismic creep (as), left-stepping en echelon cracks in pavement (ec), landslide-related cracks (lc), liquefaction (lq), lateral spreading or slumping (ls), and many other styles of ground cracking (Appendix A). The relative degree of confidence in the judgement that the earthquake produced a feature, whether related to strong ground motions or to surface-fault rupture, was ranked as follows: E1 indicates certain evidence for tectonic ground deformation; E2 indicates possible evidence for tectonic ground deformation; and E3 indicates inconclusive evidence for tectonic ground deformation. Features probably not related to tectonic movement or strong shaking are queried.

Unequivocal evidence for surface-fault rupture was rarely observed for historic earthquakes on the central Calaveras Fault. Toppozada et al. (1981) note anecdotal reports of a "fissure…near Soap Lake House on the Pacheco Pass Road [Highway 152]" attributed to an earthquake in 1897. Because the dimensions of the fissure and additional details of the surface breaks were not reported, evidence for surface-fault rupture in 1897 is uncertain. However, Cotton et al. (1979) and Armstrong (1979) reported a well-defined crack directly east of benchmark BM 160 north of San Felipe Lake (also referred to as Soap Lake) following the 1979 earthquake. This crack occurred near a probable earthquake-related fissure reported in 1897, exhibited a maximum of 6 mm of right-lateral displacement striking N 20° W, and was interpreted by Cotton et al. (1979) as surface-fault rupture. Post-seismic creep increased the offset to 10 mm within four days after the earthquake (Armstrong, 1979). Following the 1984 earthquake, "fresh cracks…extending

from older cracks" were observed at the same location and displayed 1 mm of displacement, yet Harms et al. (1984) concluded that this was insufficient evidence for surface-fault rupture.

The strongest evidence favoring a tectonic origin for surface breaks during the 1984 earthquake occurred at the southern end of Anderson Lake and in San Felipe Valley. These cracks, observed by Harms et al. (1984) and Hart (1984), displayed a northwest-southeast orientation, coincided with mapped Quaternary traces of the fault, and exhibited a component of right-lateral slip—all criteria consistent with surface faulting. However, evidence for a nontectonic origin included: (1) the absence of lateral displacement and post-seismic slip for some cracks; (2) the spatial association of some of the cracks with active landslides; (3) the limited, discontinuous nature of the surface breaks; and (4) the lack of continuity of displacement or trend for some of the cracks (Harms et al., 1984). Despite the equivocal nature of the observations, Hart (1984) preferred surface rupture as the best explanation for two parallel, northwest-trending cracks that crossed East Dunne Avenue. Harms et al. (1984) concluded that the balance of evidence did not require a tectonic explanation, but they could not preclude the possibility that the 1984 Morgan Hill earthquake produced surface-fault rupture.

Certain types of evidence for earthquake-related ground deformation accurately locate the active trace of the fault, whereas other forms of evidence may occur several meters to tens of kilometers away from the fault that ruptured. For example, surface breaks that exhibit post-seismic slip, cracks aligned with mapped Quaternary fault traces, and measured offsets showing a component of lateral slip accurately locate the fault and provide sufficient evidence for recent activity. In contrast, earthquake-induced ground failure involving liquefaction, lateral spreading or landsliding provides poor constraints on the location of active fault traces. These relations help estimate the uncertainty in the location of individual fault traces and assist in judging the Holocene (or in this case, historic) activity of particular fault traces.

2.3 Evidence for Historic Creep

Evidence for historic creep at the ground surface occurs in many places along the central Calaveras Fault and provides excellent information for accurately locating active fault traces. Sites where creep has been observed are annotated on Plates 1 and 2 by codes that refer to specific features identified in published reports for specific creep localities. The map also shows creep localities identified through field reconnaissance where new evidence for creep was found, and where alignment arrays provide a means to estimate the active creep rate through repeated surveys. Evidence for creep along the central Calaveras Fault consists chiefly of left-stepping en echelon cracks in pavement (ec) and right-laterally offset fence lines (rf) (Plates 1 and 2).

Previous evidence for creep within the nine quadrangles covered by this map has been documented by Armstrong and Wagner (1978), Armstrong et al. (1980), Nason et al., 1974, Radbruch-Hall (1974), and Rogers and Nason (1971). The U.S. Geological Survey installed two alignment arrays, one located at Coyote Ranch and another at Furtado Ranch, in 1968 and 1972, respectively (Plate 2b). Data from the Coyote Ranch array suggest a historic creep rate of 13 to 14 mm/yr punctuated by episodic acceleration in the rate of creep around the time of the 1979 Coyote Lake, the 1984 Morgan Hill, and possibly the 1989 Loma Prieta earthquakes (J. Galehouse and J. Lienkaemper, unpublished data, 1999). The existing alignment array and three

creep meter instruments at Furtado ranch were abandoned due to flooding in December of 1972 five months after they were installed. Kelson et al. (2003) resurveyed the existing alignment array and derived a creep rate estimate of about 14 mm/yr for the interval between 1972 and 2001. Also, aligned monuments established across the crest of Coyote Dam provide evidence for creep at a rate of about 12 mm/yr over a period of 21 years (Geomatrix, 1994; J. Nelson, 2003, pers. comm.).

The reliability of creep evidence is rated as follows: C1 indicates sites that provide reliable creep rate estimates; C2 indicates certain evidence for creep; and C3 indicates inconclusive evidence for creep (after Lienkaemper, 1992). Queried creep evidence may be the result of nontectonic phenomena. These ratings indicate the relative confidence that the evidence reported resulted from tectonic fault creep (C1 and C2) and not landsliding, soil creep, differential settlement, lateral spreading or other potential nontectonic causes. For example, possible fault creep damage to the spillway of Coyote dam reported by Radbruch-Hall (1974) was assigned a reliability rating of C3 because Williams et al. (1973) attributed the damage to landsliding (Plate 2a). Furthermore, Geomatrix (1994) concluded that there were insufficient data to evaluate movement on faults beneath the right abutment and spillway of Coyote dam. Offset fence lines or en echelon cracks in pavement typically were assigned a rating of C2. In contrast, the reliability rating C1 was assigned only to the alignment arrays at Coyote Ranch and Furtado Ranch.

2.4 Geological Investigations Along the Fault

The results of several geological investigations provide useful data to evaluate the activity and location of active traces along the central Calaveras Fault. There have been 34 documented trenches across the central Calaveras Fault at a total of 7 sites. Trench symbols and codes on the map depict excavations or other geological data that crossed or came to within several hundred meters of fault traces that show evidence for activity since the latest Pleistocene.

Cotton et al (1986) exposed probable Holocene traces of the fault in paleoseismic trenches excavated at Ruby Canyon and San Felipe Lake. Of the five trenches excavated southeast of Highway 152 near San Felipe Lake, four were not logged due to caving, lack of evidence for faulting, or shallow groundwater. However, one trench exposed interbedded alluvial and lacustrine deposits clearly displaced by multiple faults with apparent down-to-the-west vertical separation and stratigraphic relations suggestive of a significant strike-slip component of motion. Although no radiocarbon ages were obtained from the site, the fault trace exposed by Cotton et al. (1986) probably offsets Holocene deposits given its position on the alluvial Hollister Plain. Four trenches at Ruby Canyon exposed several shear zones in bedrock aligned with left-stepping en echelon cracks in Leavesley Road. Young (likely Holocene) alluvial deposits depicted in the log of Trench 3 appear to be displaced, but Cotton et al. (1986) provided no age estimate. No slip rate estimate was reported for either of these sites (Cotton et al., 1986).

Two fault-normal trenches at Furtado Ranch (Plate 2b), about 3 km south of the San Ysidro Creek site, exposed the active creeping trace bounding the east side of a small sag pond and an older fault bounding the west margin of the pond that showed possible evidence for Pleistocene to Holocene offset (Kelson et al., 2003). The two trenches were excavated on either side of a

U.S. Geological Survey alignment array installed in 1972, that has been displaced by the primary fault trace at a creep rate of about 14 mm/yr.

Two of five trenches excavated along the southern boundary of the Pacheco Pass landfill showed evidence for two secondary faults southwest of the primary fault trace identified at Furtado Ranch (EMCON Associates, 1990). The sense of displacement on the faults was inferred to be right-lateral oblique reverse based on trench exposures that showed northeast-dipping fault planes. The report by EMCON Associates (1990) did not include data to assess the most recent movement of the secondary faults.

The most reliable constraints on the location and late Holocene geologic slip rate of the central Calaveras Fault come from extensive paleoseismic investigations at San Ysidro Creek, east of Gilroy. Baldwin et al. (2002) and Kelson et al. (1998) excavated five fault-normal and six fault-parallel trenches across the primary active trace of the fault that expose six to eight offset stream channels (Plate 2b). Measurements of cumulative right-lateral displacement of the oldest four paleochannels provide a slip rate estimate of 8 to 19 mm/yr (Baldwin et al., 2002).

Trenches and outcrops in the vicinity of Coyote Dam (Marliave, 1936; Geomatrix, 1994) located the creeping trace of the fault and provide evidence for transpressional and transtensional displacement of Plio-Pleistocene deposits and possibly Quaternary terrace gravels (Plates 2a and 2b). Exploratory trenches, a test pit, and a tunnel excavated during construction of the dam document two fault traces through the left (east) abutment and faults of unknown age in the right (west) abutment (Marliave, 1936). Periodic measurements of an alignment array across the crest of the dam show evidence for active creep on both faults in the left abutment (Geomatrix, 1994).

We reviewed twenty-four reports from fault investigations carried out to satisfy the Alquist-Priolo (AP) Earthquake Fault Zoning Act of 1972 (Hart and Bryant, 1997). Most AP studies that we reviewed involved reconnaissance geologic mapping, literature review, and interpretation of aerial photography. A few reports included the results of shallow seismic reflection profiles, magnetometer surveys and trenching. Only one AP report (JCP—Engineers & Geologists, Inc., 1987) contained equivocal evidence (Th?) for Holocene faulting in a trench across an apparent secondary trace of the Calaveras Fault near Felter Road (Plate 1a).

2.5 Quaternary Surficial Deposits

Mapping of Quaternary surficial deposits involved the interpretation of 1:24,000-scale topographic maps and aerial photography, published and unpublished geologic maps, and field reconnaissance. Documentation of mapping procedures and data sources is shown in Table 2. The ages and environments of the deposits and their geologic unit descriptions are modified from Knudsen et al. (2000), with the exception of deposits of late and middle Pleistocene age. In this study, the late Pleistocene age category refers to deposits younger than 125,000 years old but older than 11,000. Deposits of early to middle Pleistocene age range from 125,000 to 2 million years old. The conventional age assignments were adopted because of the lack of sufficient age data to resolve Pleistocene deposits between 30,000 and 11,000 years old from deposits as old as 125,000 years. Otherwise, the geologic mapping followed the standard procedure outlined by Knudsen et al. (2000).

Table 2. Documentation of mapping procedures and data sources

7.5-minute quadrangle	Mapping procedure and data sources
Calaveras Reservoir, San Jose East, Mt. Day, Lick Observatory	Interpretation of topographic contours, field reconnaissance and aerial photography dating from 1939 and 1940 (U.S. Department of Agriculture, CIV series, 1:20,000-scale) and 1999 (WAC Corp., WAC-C-99CA series, 1:24,000-scale). Previous mapping reviewed includes: Bryant, 1981a; Cotton, 1972; Dibblee, 1973; Dibblee, 1972a; 1972b; Helley and Graymer, 1997; unpublished mapping by D.G. Herd; Knudsen et al., 2000; Radbruch-Hall, 1974; Wentworth et al., 1999.
Morgan Hill, Mt. Sizer	Interpretation of topographic contours, field reconnaissance and aerial photography dating from 1939 (U.S. Department of Agriculture, CIV series, 1:20,000-scale) and 1999 (WAC Corp., WAC-C-99CA series, 1:24,000-scale). Previous mapping reviewed includes: Bryant, 1981b; Cotton, 1972; Dibblee, 1973d; 1973e; Radbruch-Hall, 1974; Wentworth et al., 1999.
Gilroy, Gilroy Hot Springs	Interpretation of topographic contours, field reconnaissance and aerial photography dating from 1939 (U.S. Department of Agriculture, CIV series, 1:20,000-scale) and 1999 (WAC Corp., WAC-C-99CA series, 1:24,000-scale). Previous mapping reviewed includes: Armstrong and Wagner, 1978; Dibblee, 1973b; 1973c; Nakata, 1980; Radbruch-Hall, 1974; Smith, 1981; Wentworth et al., 1999.
San Felipe	Interpretation of topographic contours, field reconnaissance and aerial photography dating from 1939 (U.S. Department of Agriculture, CIV series, 1:20,000-scale), 1999 and 2000 (WAC Corp., WAC-00-CA series, vertical, stereo, black and white, 1:24,000-scale). Previous mapping reviewed includes: Bryant, 1981c; Dibblee, 1975; Radbruch-Hall, 1974; Rogers, 1973.

Surficial deposits can be identified based on landform shape and relative geomorphic position, crosscutting relations and superposition, and deposit texture, sorting and sedimentary structure. Landforms, including stream channels and terraces, alluvial fans, fan levees, and shallow basins, were delineated by interpretation of topographic maps and aerial photography flown in 1939, 1940 and 1999. The criteria used to evaluate deposit age includes: (1) soil profile development; (2) relative degree of surface dissection or other surface modification; (3) relative topographic

position; (4) correlation to dated deposits in the region; and (5) correlation to the stratigraphic framework used by previous researchers (e.g., Atwater et al. 1977; Helley et al., 1979; Atwater, 1982; Knudsen et al., 2000). Deposits that could not be confidently distinguished as either Holocene or Late Pleistocene were assigned the age designation of Late Pleistocene to Holocene. This designation is also used where Holocene deposits are inferred to interfinger with or form a thin veneer (< 5-feet thick) over late Pleistocene deposits.

2.6 Landslides

Large landslides delineated on the map were modified from the compilation of Wentworth et al. (1999). These landslides represent Quaternary surficial deposits greater than 200- to 300-m wide that are composed principally of bedrock displaced by sliding. The map does not show smaller landslides, debris flows, earth flows or areas subject to solifluction restricted to less than 200 m across, nor is the map a comprehensive representation of landslide hazards. A more thorough and detailed depiction of landslides was not included on this map because (1) landslides, although likely Quaternary in age, are rarely useful in assessing the recency of Holocene fault activity; (2) the overwhelming abundance of landslides, that in some areas of the map occur away from active fault traces, shift the focus of the map away from relevant relations between other surficial deposits and active fault traces; and (3) 1:24,000-scale landslide mapping was not part of the scope of this project. For a more comprehensive treatment of landslides in Santa Clara County, refer to Nilsen et al. (1975). Landslides and deposits formed by other mass-wasting processes may locally modify, obscure or completely remove tectonically sculpted landforms. On Plates 1 and 2 specific codes (e.g., G3, ls) indicate where landslides appear to influence the geomorphic expression of active fault traces. Where landslides hide evidence for active faulting, the fault trace is indicated by a dotted, and in some cases, queried line. Other map codes (e.g., E2, lc) indicate sites of earthquake-related ground deformation interpreted as seismically triggered landsliding.

3.0 STYLES AND GEOMETRY OF ACTIVE FAULT TRACES

Various styles of deformation within a fault zone and the overall complexity of its active traces reflect local variations in the strain field near the fault. Such variations in the surficial traces of the fault may delineate discrete structural elements that influence historical seismicity patterns. Fault segments control the overall length of rupture, which relates to the maximum earthquake magnitude the fault is capable of generating. Changes in the geometry of the surface trace of the central Calaveras Fault that may reflect where fault rupture initiates and ends include right-releasing stepovers and left-restraining bends characterized by marked changes in the strike of the fault (Aydin and Nur, 1985; Lettis et al., 2002). The near surficial architecture of the central Calaveras Fault exhibits classic fault geometries consistent with both transpressional and transtensional styles of deformation. The following discussion characterizes seven sub-sections of the central Calaveras Fault that exhibit unique styles of geomorphic expression, varying degrees of continuity, different widths of the deformation zone, changes in overall strike of the zone, and geometries that consist of both right-releasing stepovers, left-stepping en echelon faults within a releasing bend, and left-restraining double bends along the fault. Such characteristics can be used to evaluate fault segments and segmentation models. The seven sub-sections of the central Calaveras Fault are described below, from north to south.

3.1 Fault-related Features at Calaveras Reservoir

At the northern end of the central Calaveras Fault, strain is transferred to the northwest through multiple north-striking en echelon fault traces across a 1- to 1.5-km-wide, 5-km-long asymmetric depression currently filled by Calaveras Reservoir (Plate 1a). West-facing scarps, right-laterally offset streams and steep faceted ridges on the southeast side of the depression are consistent with dextral displacement with a down-to-the-west normal component of slip. Simpson et al. (1992) previously characterized a significant change in strike of the primary fault zone as a 7-km-long right-releasing double bend, and WGCEP (1999) and Kelson (2001) denote this double bend as a major segment boundary between the northern and central segments of the Calaveras Fault.

We characterize the Calaveras Reservoir region as a complex right-releasing fault bend evident as a 27° to 29° change in strike of the primary fault zone toward the northwest. Deformation across the region involves multiple left-stepping, en echelon, north-trending secondary faults that lie beneath Calaveras Reservoir and appear to accommodate right-lateral oblique-normal slip. Several lines of evidence suggest that this region acts as a segmentation boundary between the northern and southern sections of the fault, including: (1) a significant change in strike (27° to 29°) of the primary fault zone; (2) marked differences in estimated geologic slip rates and geodetic creep rates between the northern and central sections of the fault (Kelson, 2001; WGCEP, 1999); and (3) structural complexity related to transfer of strain to the southern Hayward Fault evident as the Mission Peak seismicity trend (Andrews et al., 1993; Wong and Hemphill-Haley, 1992).

3.2 Fault-related Features Between Calaveras Reservoir and Halls Valley

To the south of Calaveras Reservoir, the fault traverses steep, high relief terrain. Along the 12-km-long sub-section of the fault between Calaveras Reservoir and Halls Valley, dense vegetation and landslides obscure much of the fault. Geomorphic expression of the fault is concentrated along a narrow (250- to 500-m-wide) laterally continuous zone that trends N 35° W to N 37° W. Evidence for Holocene activity of the primary and secondary traces of the fault occur along Felter Road in fault trenches excavated for an Alquist-Priolo study (JCP, 1987). Left-stepping en echelon cracks attributed to creep cross Felter Road from the southeast to the northwest approximately 200-km southeast of the Alquist-Priolo study site (Plate 1a). Northwest of Cherry Flat Reservoir, 1- to 1.5-km of dextral displacement of Upper Penitencia Creek attests to long-term slip on the fault during the late Pleistocene.

The 1988, M 5.1 Alum Rock earthquake, located 1.5 km south of Cherry Flat Reservoir, occurred adjacent to a 0.5- to 0.7-km-wide right stepover along the fault 2.5 to 3 km north of Halls Valley, informally named the Aguague stepover. Northwest trending linear tributaries of Arroyo Aguague are joined obliquely by north-trending lineaments that define an elongate rhomboid approximately 2.7 km long directly south of the 1988 epicenter. We interpret the northwest-trending lineaments as a right stepover of the primary active fault trace connected by a potentially active north-trending secondary fault. This association of M >5 earthquakes with a macroscopic change in the surface geometry of active fault traces occurs elsewhere along the central Calaveras Fault and may provide insight regarding fault segmentation models.

3.3 Fault-related Features Between Halls Valley and San Felipe Valley

At Halls Valley, the fault zone includes a 1-to-1.5-km-wide releasing stepover and small pull-apart basin (Plate 1b). Discontinuous, subparallel lineaments northwest of Halls Valley are well defined along Arroyo Aguague. Southeast of Arroyo Aguague, a broad (1.5-km-wide) fault zone contains three distinct series of lineaments that span the valley and a fourth series of less conspicuous, discontinuous geomorphic features east of Halls Valley. A north-trending graben containing several sag ponds, aligned tonal and vegetation lineaments, and springs bound the northwestern margin of Halls Valley (Figures 4a and 4b**)**. We observed no evidence for active surface creep where the graben intersects old fence lines and Mt. Hamilton Road. Lineaments associated with this graben continue southward along less distinct linear valleys and ridge-top saddles to intersect a prominent side-hill trough that trends N 36° W in the hills along the western edge of Halls Valley. This pronounced linear valley also contains several closed depressions and is aligned with well-defined lineaments to the south that merge with active fault traces at San Felipe Valley. Although this prominent geomorphic feature parallels the strike of local bedding and may be modified by landsliding, its strong geomorphic expression and alignment with active fault traces to the south suggest that it may be an active trace bordering the western margin of Halls Valley.

Northeast of Halls Valley Lake, a series of well-defined and continuous fault-related lineaments include linear troughs and southwest-facing scarps, a spring, a right-laterally offset ravine and bedrock of different Franciscan lithologies juxtaposed along a fault. These features border the northeastern margin of Halls Valley Reservoir that occupies a large closed depression. In the vicinity of the lake, our reconnaissance surveys of old fence lines and paved roads that crossed prominent mapped lineaments showed no sign of active surface creep. Southeast of the lake, active traces are evident as linear drainages and southwest-facing scarps that define the northeastern margin of Halls Valley. The geomorphic expression becomes progressively better defined and continuous at the southeastern end of the valley where San Felipe Creek follows a southeast-trending, 2-km long linear valley incised into bedrock.

Less conspicuous, discontinuous features define two additional potentially active fault traces in Halls Valley. Evidence for an active trace that may run up the center of the valley include a linear stream channel aligned with weakly-expressed northwest-trending vegetation and tonal lineaments and a southwest-facing scarp in bedrock west of Halls Valley Reservoir. To the east of the valley, discontinuous, poorly expressed linear drainages aligned with closed depressions, deflected and offset creek channels, and uphill- (east-) facing scarps provide evidence for a fourth active fault trace within the 1.5-km-wide fault zone. The spatial association of several of these features east of Halls Valley with the epicenter of the 1984 M 6.2 Morgan Hill earthquake also suggest recent activity (Plate 1b).

Southeast of Halls Valley, the Madrone Springs Fault appears to be dismembered by active traces of the Calaveras Fault. The Madrone Springs Fault structurally juxtaposes the Upper-to Middle Miocene Briones and Claremont Formations against Franciscan melange in the Diablo Range (Wentworth et al., 1999). The fault strikes nearly 30° more westerly than the regional

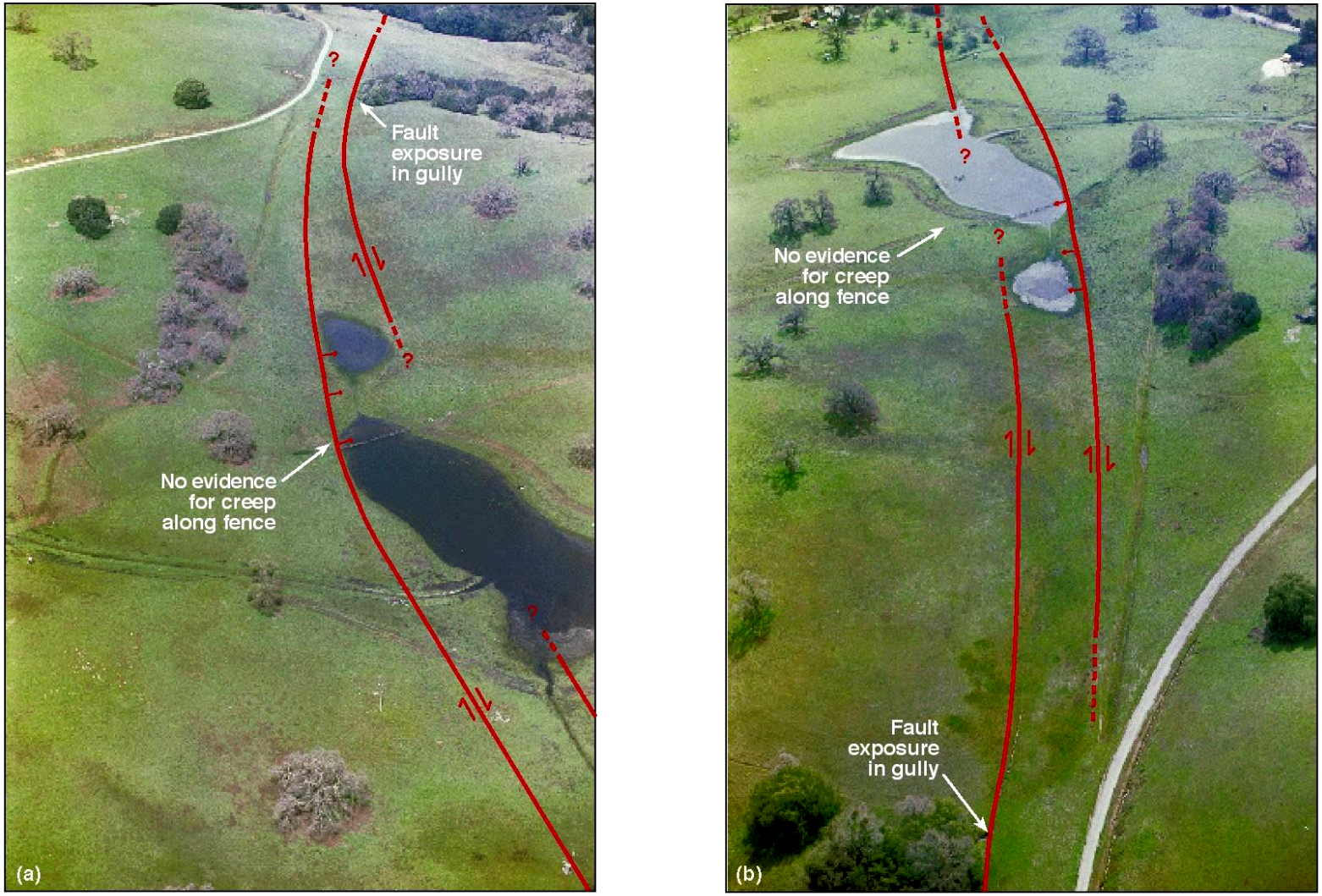

Figure 4. Oblique aerial photographs of the secondary fault strand at Halls Valley site, showing ephemeral sag ponds. Photographs taken on March 25, 2002, during relatively wet field conditions. (a) Looking north, (b) looking south.

strike of the Calaveras Fault. Between San Felipe and Halls Valleys the Calaveras Fault appears to right-laterally offset the Madrone Springs Fault by 10 to 15 km.

3.4 Fault-related Features Between San Felipe Valley and Anderson Lake

Active fault traces delineate a 5-km-long double bend across a 1.5- to 2-km-wide right-releasing stepover at San Felipe Valley (Plate 1b). This stepover was recognized by King and Nábêlek (1985). Tonal lineaments, linear stream channels, and scarps trend N 4° W to N 12° W over a relatively narrow area (250- to 500-m wide) confined within the valley. North of San Felipe Valley, the primary trace of the Calaveras fault follows San Felipe Creek and takes a sharp 20° to 23° bend about 1 km southwest of the epicenter of the 1984 earthquake (Plate 1b). Possible fault-related lineaments west of San Felipe Creek near Panochita Hill bend toward the west parallel to the regional fault strike and, if active, define a 20° to 24° change in fault strike. South of the valley, the primary fault zone bends 16° to 24° to the southeast and parallels Las Animas Creek.

Earthquake-triggered movement on several cracks observed in San Felipe Valley following the 1984 Morgan Hill earthquake (Harms et al., 1984) provides equivocal evidence for surface fault rupture. However, repeated measurements of quadrilateral arrays set up across two sets of cracks aligned with two mapped fault traces within days of the earthquake showed no indication of post-seismic creep (Brown, 1987; Harms et al., 1984). No other evidence for surface fault creep has been reported in the San Felipe Valley.

Interpretation of gravity data suggests the presence of a 0.7-km-wide, 1.3-km-long, 40-m-deep north-trending rectangular basin beneath San Felipe Valley (Chuang et al., 2002). An inferred fault bordering the western side of the basin coincides with several previously unrecognized geomorphic lineaments that cut across Holocene alluvial fans and may suggest recent fault activity (Plate 1b). This observation suggests that geomorphic lineaments along the western margin of the valley that continue northward toward Panochita Hill represent an active western trace of the fault. Chuang et al. (2002) conclude that limited offset has occurred on the Central Calaveras fault compared to other San Andreas system faults based on the restricted size, shallow depth and relative young age of the alluvial basin.

Between San Felipe Valley and Anderson Lake, several possible fault-related geomorphic features are well expressed along a 0.5- to 1-km-wide zone that becomes progressively wider toward the southeastern end of Anderson Lake (Plate 2a). Along this 12-km-long section, the fault strikes between N 31° W and N 35° W. Middle to late Pleistocene terraces along lower San Felipe Creek originally were deposited by a stream flowing from Packwood Valley that has since experienced 4 km of right-lateral offset by the central Calaveras Fault (Harden and Gallego, 1992). Several apparently active fault traces dissect a small remnant ridge top where lower San Felipe Creek sharply turns westward and crosses the fault (Plate 2a). The primary trace of the fault takes a left-restraining step across this hill suggesting that locally the fault may exhibit a reverse component of slip. The eroded ridge may be a pop-up structure bound by reverse faults to the southwest and northeast (Plate 2a). To the east, north-trending lineaments including distinct faceted ridges, linear troughs and slope breaks run parallel to San Felipe Valley and may

form the southeastern margin of a large, incipient rhomboid-shaped discontinuity in the fault (Plate 2a).

3.5 Fault-related Features Between Anderson Lake and Coyote Dam

Northeast of Anderson Lake, the fault zone consists of multiple, subparallel and arcuate traces characterized by ponded alluvial basins, shutter ridges, closed depressions, right-laterally offset drainages, linear troughs, side-hill trenches, and scarps. At the southeastern end of Anderson Lake a complex zone of north-trending arcuate valleys containing small lakes and ponds are influenced by landsliding (Plate 2a). Active traces of the fault in this area likely are modified or obscured by tectonically controlled slide-related landforms. Earthquake-triggered slip on cracks across East Dunne Avenue (Harms et al., 1984; Hart, 1984) east of the lake demonstrates that these features are spatially associated with active traces of the fault. Additional evidence for fault activity in this area includes earthquake-related displacement and possible creep through the southern abutment of Cochrane Bridge (Mathieson, 1984) and probable earthquake-related landslide cracks 300- to 400-m west of the bridge (Harms et al., 1984).

Along Coyote Creek between Anderson Lake and Coyote Dam, the main trace of the fault strikes N 43° W, the most westerly strike observed anywhere along the fault. Geomorphic lineaments along Coyote Creek are continuous and well expressed laterally over a distance of 4 km and concentrated within a 100- to 400-m-wide zone. The more westerly strike of the fault marks an 11° to 13° departure from the regional strike of the fault to the north and south that defines a left-restraining double bend. The surficial geometry of the fault appears to reflect a clear left-restraining overlap in microseismicity relocated by Schaff et al. (2002) and is spatially associated with the southeastern limit of aftershocks following the Morgan Hill earthquake (Bakun et al, 1984).

Trenches and geologic exposures examined by Geomatrix (1994) north of Coyote Dam revealed evidence for historic surface fault displacement (creep) of alluvium deposited after dam construction in 1936. In addition, these trenches exposed right-lateral, oblique-reverse secondary faults that offset Plio-Pleistocene deposits and possibly late Quaternary terrace gravels. Evidence for transpressional faulting observed north of the dam along Coyote Creek is consistent with the left-restraining geometry defined by active fault traces that strike more westerly (N 43° W) than the regional (N 30° W) strike of the fault (Plate 2a).

3.6 Fault-related Features Between Coyote Dam and San Ysidro Creek

Coyote Lake occupies a 6-km-long, northwest-trending valley within a 0.5- to 1-km-wide right-releasing stepover inferred to be a pull-apart basin (Aydin and Page, 1984) (Plates 2a and 2b). Repeated measurements of monuments across Coyote Dam, operated by Santa Clara Valley Water District, provide a preliminary creep rate estimate of about 12 mm/yr on one or two active fault traces beneath the left abutment of the dam (Geomatrix, 1994; J. Nelson, 2003, pers. comm.). Directly south of the dam, a series of well-defined scarps, linear troughs, and offset streams project across the lake to several well-defined faceted ridge spurs on the northeastern shore (Plate 2a). Looking toward the southeast, the fault steps right from the northeastern shore, across the central part of the lake, to the southwestern shore and continues to the southeast

laterally displacing a flight of highly dissected Pleistocene fluvial terraces (Plate 2b). In addition to historic fault creep through the dam embankment, evidence for fault activity includes a right-laterally offset fence line, several right-laterally offset or deflected creeks, and an alignment array located south of the lake installed by the U.S. Geological Survey in 1968 (Plate 2b). The epicenter of the 1979 Coyote Lake earthquake was located approximately 1.5 km northeast of the lake.

Exploration trenches, test pits and a tunnel excavated during foundation design and construction at the left abutment of the Coyote Dam exposed two traces of the Calaveras Fault (Marliave, 1936). Both traces dip steeply to the west, bound both sides of a resistant serpentinite knob, and place Miocene and younger rocks on the west adjacent to Cretaceous rocks of the Berryessa Formation on the east. Although no Holocene deposits were present in these exposures, possible displacement of Quaternary alluvium observed in exploration trenches along the dam axis and certain evidence for historic creep across the embankment alignment array provide sufficient evidence for fault activity Geomatrix, 1994). Faults that offset rocks of the Berryessa Formation were identified in exploration trenches during dam construction at the right abutment (Marliave, 1936). In a geotechnical evaluation of landslide potential at the dam, Geomatrix (1994) concluded that there were insufficient data to evaluate the age and style of the most-recent movement on northwest striking, southwest dipping faults in the right abutment.

The main active fault trace and several secondary transtensional faults were identified in outcrops and a trench south of the dam (Geomatrix, 1994). The trench, excavated across a prominent linear trough and west-facing serpentinite scarp, exposed a complex fault zone that offsets clayey gravel and sand deposits of unknown age. Geomatrix (1994) interpreted this fault as the active creeping trace based on geomorphic expression and possible fractures that appeared to break the ground surface. North- to northeast-striking secondary faults with apparent down-to-the-west separation documented by Geomatrix (1994) are consistent with the kinematic model that Coyote Lake occupies a pull-apart basin formed in an extensional stepover.

A prominent wind gap at the headwaters of Skillet Creek southwest of Coyote Lake suggests that at one time Coyote Creek flowed to the west supplying sediment to a large Pleistocene alluvial fan complex in the eastern Llagas Valley east of Gilroy. Several west- to southwest-flowing creeks supplying sediment to these fans today appear to be beheaded near the ridge crest west of Coyote Lake including, from north to south, New Creek, Church Creek, Skillet Creek and Oak Creek. The creek channels and the Pleistocene fans appear to be oversized compared to the corresponding watershed areas suggesting that these creeks may be former channels of Coyote Creek that have since been offset by the Calaveras Fault.

A narrow zone (100- to 400-m-wide) of well-defined scarps, side-hill benches and linear troughs delineate the primary active fault trace between Coyote Lake and San Ysidro Creek (Plate 2b). Along this 6- to 8-km-long section the fault is very straight and has a consistent strike between N 29° W and N 31° W. Geological evidence for Holocene slip and historic creep along this section of the fault is abundant. For example, several fence lines appear to be offset in the area (Armstrong and Wagner, 1978; Armstrong et al., 1980) and left-stepping en echelon cracks cross Leavesley Road in many places; some of these cracks slipped coseismically during the 1979 Coyote Lake earthquake (Armstrong, 1979) (Plate 2b). Paleoseismic trenches locate the fault at

Ruby Canyon and San Ysidro Creek where Holocene deposits are clearly displaced (Baldwin et al., 2002; Cotton et al., 1986; Kelson et al., 1998). A large closed depression at Ruby Canyon appears to be related to ponding of alluvial sediment caused by the apparent 500- to 600-km, right-lateral offset of Alamias Creek.

3.7 Fault-related Features Between San Ysidro Creek and San Felipe Lake

The southern limit of the central Calaveras Fault is interpreted to be at San Felipe Lake and is marked by a 6° to 9° restraining bend (Plate 2b). This restraining geometry imposes contraction northwest of the lake expressed as west-northwest-trending scarps and slope breaks inferred to be reverse faults near the Pacheco landfill. Deformation occurs across a zone approximately 1-km wide. Right-laterally offset fence lines observed across the primary fault trace and across two inferred dextral-oblique-thrust faults to the west (Armstrong et al., 1980) provide evidence for active creep on multiple fault strands. Measurements of an alignment array installed in 1972 at Furtado Ranch also document historic creep on the primary fault trace (Kelson et al., 2003). Paleoseismic trenches at Furtado Ranch and along Highway 152 near San Felipe Lake (Plate 2b) confirm Holocene displacement on the main fault north of San Felipe Lake (Cotton et al., 1986; Kelson et al., 2003). Earthquake-triggered cracking and post-seismic creep were observed across Highway 152 as a result of earthquakes in 1897, 1979 and 1984 (Cotton et al., 1986; Armstrong, 1979; Harms et al., 1984; Toppozada et al., 1981).

4.0 RELATIONSHIP BETWEEN SURFACE FAULT GEOMETRY AND HISTORIC EARTHQUAKE RUPTURE

Studies of the lateral extent of historic earthquakes document correlations between the initiation or termination points of fault rupture and bends or en echelon steps in the surficial expression of a fault (Bakun, 1980; King and Nábêlek, 1985; Lettis et al., 2002). The epicenters and inferred rupture lengths of four earthquakes on the central Calaveras Fault (Oppenheimer et al., 1990) are spatially associated with steps or bends defined by active fault traces (Figure 2). This relationship implies that the surficial pattern of the central Calaveras Fault reflects geometric or rheological barriers to rupture propagation at depth.

The 1979 Coyote Lake (M 5.9) earthquake initiated near a right-releasing stepover that has created a rhomboid-shaped pull-apart basin occupied by Coyote Lake (Aydin and Page, 1984). The main shock occurred at the latitude of Coyote Lake and ruptured to the south (Oppenheimer et al., 1990). Although King and Nábêlek (1985) suggested that aftershocks following the Coyote Lake event ended near a change in fault strike, detailed mapping of this area delineates a very straight fault with no significant geometric anomalies near the southern limit of rupture (Figure 5).

The 1988 Alum Rock (M 5.1) earthquake epicenter also is spatially associated with a right step in the fault (Plate 1a). The epicenter of this event occurred near the northeastern apex of 2.7-km-long, 0.5- to 0.7-km-wide rhomboid-shaped arrangement of active fault traces about 5 km northwest of Halls Valley near Cherry Flat Reservoir (Plate 1a). The high topography and lack of obvious evidence for extension across the stepover suggests that this relatively small discontinuity along the fault may be an incipient feature.

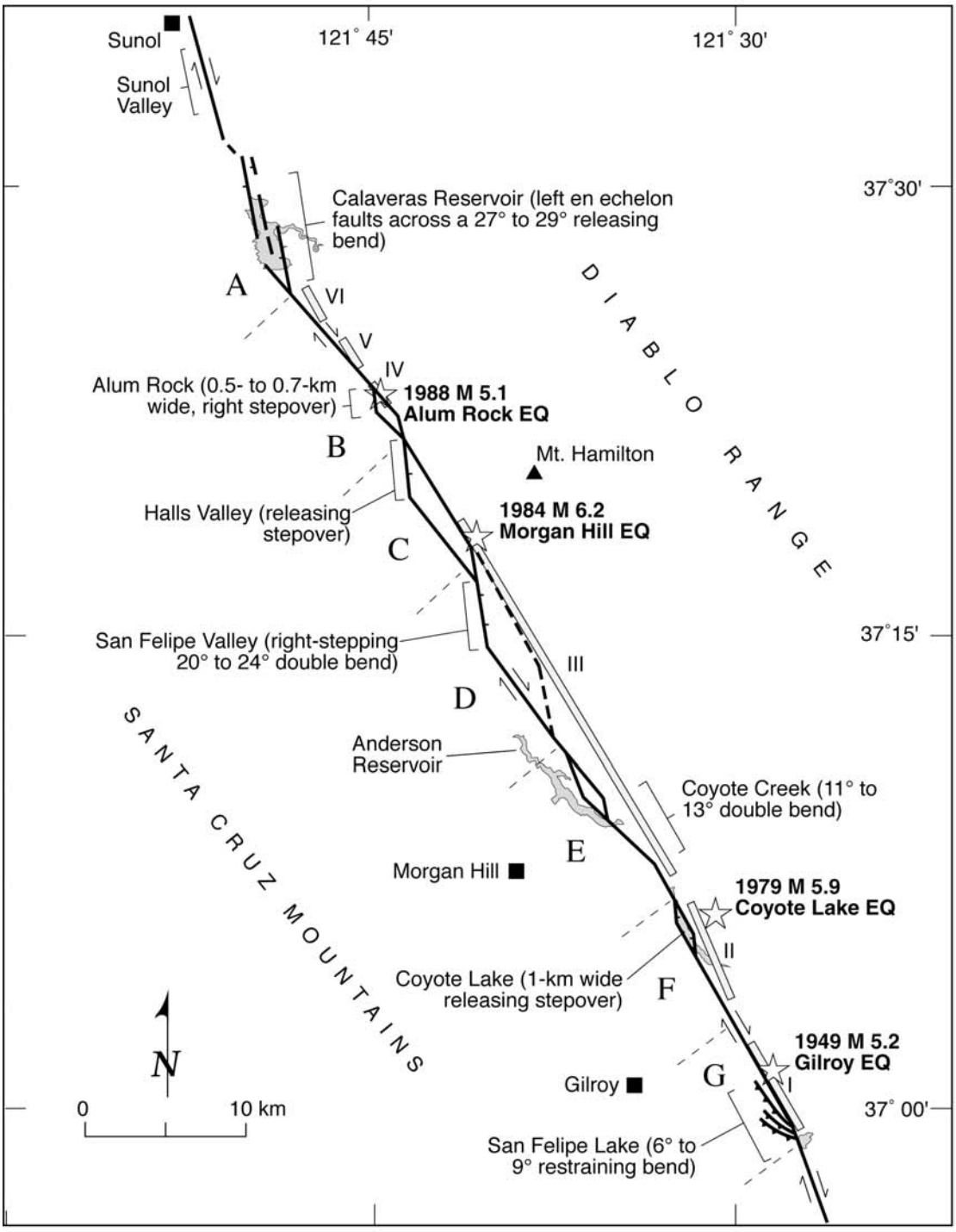

Figure 5. Kinematic model showing geometric relations among extensional stepovers as well as releasing and restraining bends defined by active traces of the central Calaveras fault. Historic earthquake epicenters and inferred rupture lengths from Oppenheimer et al. (1990). Bold letters represent seven sub-sections of the fault, delineated by thin dashed lines, that exhibit unique styles of geomorphic expression, and various geometric patterns that appear to correlate with historic earthquake fault rupture. The seven sub-sections discussed in the text include: A, Calaveras Reservoir segment boundary; B, Calaveras Reservoir to Halls Valley; C, Halls Valley to San Felipe Valley; D, San Felipe Valley to Anderson Lake; E, Anderson Lake to Coyote Dam; F, Coyote Dam to San Ysidro Creek; G, San Ysidro Creek to San Felipe Lake.

The 1984 Morgan Hill (M 6.2) earthquake initiated near a 20° to 23° bend in the fault north of San Felipe Valley, a north trending fault-bounded basin that coincides with a 1.5- to 2-km wide right-releasing stepover in the primary active fault trace (Plate 1b). Like the Coyote Lake event, the Morgan Hill epicenter appears to be spatially associated with a rhomboid-shaped extensional basin (Chuang et al., 2002). Fault rupture terminated near the southern end of Anderson Lake near a left-restraining double bend north of Coyote Dam. This 11° to 13° change in surficial fault strike coincides with a prominent left step in relocated microseismicity at depths of 2 to 8 km (Schaff et al., 2002). Bakun et al. (1984) and Beroza and Spudich (1988) also recognized this relationship between rupture termination and change in fault strike.

The epicenter of the 1949 Gilroy (M 5.2) earthquake is located near the northern extent of a zone of inferred dextral-oblique thrust faults in the San Ysidro Hills east of Gilroy that diverge from the primary strike-slip trace of the Calaveras Fault (Plate 2b). If the 1949 rupture zone filled the aseismic region north of San Felipe Lake ("stuck patch" I in Figure 2) identified by Oppenheimer et al. (1990), then its southern termination occurred at a prominent 6° to 9° bend in the principle trace of the fault. This change in the strike of the fault represents the southern end of the central Calaveras Fault.

5.0 IDENTIFICATION OF PALEOSEISMIC RESEARCH SITE

A fundamental question that should be addressed by future research along the central Calaveras Fault is whether north-striking secondary faults reflect aseismic creep across a complex right-stepping fault system, or coseismic rupture produced by large (**M**≥6.5) earthquakes. In the northwestern part of Halls Valley, three northwest-striking traces of the Calaveras Fault are parallel with Arroyo Aguague in the vicinity of a large reservoir (Figures 4a and 4b) A secondary strand west of the reservoir strikes almost due north and is characterized by sag ponds within a closed linear depression (Figures 4a and 4b). We postulate that slip transfers between the western and eastern sides of Halls Valley along this secondary structure. This site is well suited to address the research question stated above for three reasons: (1) the secondary fault strikes approximately 35° to 40° clockwise from the strike of the regional, primary trace of the fault; (2) youthful geomorphic features delineate the fault and attest to recent movement, including a 1.5- to 2-m-high, east-facing fault scarp, a closed depression within an elongated north-trending graben, ground water springs, and tonal and vegetation lineaments and; (3) there is no historical evidence for or documentation of displaced cultural features that would indicate aseismic creep on the secondary fault (or on any other secondary structure within the Calaveras fault zone that is obliquely oriented with respect to the regional fault trend).

We propose to trench across the secondary fault strand along the northwestern margin of Halls Valley, which is interpreted as an active secondary fault bordering the northwestern margin of the 1- to 1.5-km-wide pull-apart basin in the central Calaveras fault (Figure 2). The strike of the secondary fault (N1°W to N4°E) is oriented 35° to 40° clockwise from the strike of the more linear and continuous fault trace inferred to follow Arroyo Aguague. Although geologic maps of the fault (Cotton, 1972; Dibblee, 1972; Radbruch, 1968) do not depict a single active trace through Halls Valley (Figure 2), geomorphic lineaments and possible fault-related landforms delineate multiple inferred fault strands that trend predominantly N35°W (Figure 3). The

secondary fault likely releases extensional strain as slip is transferred across Halls Valley within the right step-over in the Calaveras fault zone.

The north-trending secondary fault exhibits distinctive fault-related geomorphology, including an elongate linear trough or graben, ground water seeps, prominent vegetation lineaments, and an east-facing scarp (Figures 4a and 4b). On the basis of interpretation of aerial photography and site reconnaissance conducted during our FY2001 NEHRP research, late Holocene to historical surficial deposits overlie the fault strand (Figures 4a and 4b). These deposits may provide stratigraphic and structural information related to the earthquake history of the central Calaveras fault. Bedrock likely is shallow (<3 m) because Franciscan sandstone crops out in the ridges directly east and west of the depression (Dibblee, 1972).

A 1.5- to 2-m-high east-facing scarp on the west and a distinct vegetation lineament and series of ground water seeps on the east bind the prominent linear depression that defines the secondary fault (Figures 4a and 4b). The elongated trough is about 500-m long, 30- to 60-m wide tapering to the north. Two small ephemeral ponds seasonally occupy the closed depression. The depression presently receives colluvial sediment from the east-facing scarp bordering the western margin. Fine-grained lacustrine (pond) sediment fills the central and southern parts of the depression, and during the wettest years may be deposited across the entire length of the trough. During the dry season when ground water is low, the ponds recede and much of the depression is covered with grasses and marsh vegetation.

Two cultural features that cross the secondary fault at the Halls Valley site show no evidence for deformation due to aseismic creep. The first feature, an old pasture fence, crosses the closed depression at an angle approximately orthogonal to the fault and bisects the northern tip of the larger of two sag ponds (Figures 4a and 4b). During field reconnaissance, we investigated this fence for evidence of fault creep (e.g., right-laterally offset fence line) and found none. The second feature, Mt. Hamilton Road, obliquely crosses the secondary fault approximately 450-m south of the proposed trench sites (Figures 4a and 4b). We walked along Mt. Hamilton Road for several hundred meters on either side of the projected fault crossing and observed no sign of buckling, left-stepping en echelon cracking, or distortion of pavement, or right-laterally offset curbs or painted road lines. Similarly, we found no evidence for vertical separation across these cultural features that might indicate aseismic creep on a transtensional fault.

6.0 DISCUSSION

The map presented here identifies seven geometric sub-sections of the central Calaveras fault based on different degrees of continuity and width of the deformation zone, changes in strike of the principal fault zone, and transtensional and transpressional fault geometries. Five sub-sections are spatially correlated with rupture initiation and termination of historic M >5 earthquakes. These five sub-sections include, from north to south, the Alum Rock releasing stepover, the San Felipe Valley releasing-double bend, the Coyote Creek restraining-double bend, the Coyote Lake releasing stepover, and the San Felipe Lake restraining bend. A sixth major discontinuity not associated with historic seismicity includes north-trending en echelon faults in the vicinity of a 27° to 29° releasing bend at Calaveras Reservoir. This area is directly north of an inferred locked patch of the fault identified by Oppenheimer et al. (1990) as a likely

focal point for the next earthquake. Halls Valley, which occupies a pull-apart basin within a 1- to 1.5-km wide releasing stepover, also is not spatially associated with historic fault rupture. Multiple fault splays and arcuate, north trending lineaments east of Anderson Lake represent an additional area of geometric complexity among active surface faults.

A repeating pattern observed in the organization of active traces along the central Calaveras Fault includes north to north-northwest striking primary and secondary fault traces that appear to define geometric subsegments of the fault zone (Figure 5). Many of the north-striking structures bound the northwestern or southeastern margins of pull-apart basins and rhomboid-shaped arrangements of fault traces. Others occur within major deviations from the regional strike of the fault zone. These more northerly striking faults likely accommodate right-lateral oblique-normal motion because they exhibit a releasing geometry with respect to the regional strain direction. Thus, the overall pattern of faulting along the central Calaveras fault consists of a series of small pull-apart basins bordered by generally north-striking oblique-normal faults, separated by relatively linear, narrower northwest-trending fault reaches. From north to south, the pull-apart basins include (Figure 5): Calaveras Reservoir, Alum Rock stepover, Halls Valley, San Felipe Valley, and Coyote Lake.

Along the central Calaveras Fault, several north-striking faults serve as kinematic links between subsegments of the fault zone that strike predominantly northwest (Figure 2). For example, north-striking faults in San Felipe Valley cross a 1.5- to 2-km-wide releasing stepover connecting northwest-striking subsegments of the fault (Figure 2; Plate 1b). Another example is at Calaveras Reservoir, where en echelon, north-striking faults accommodate slip across a 27° to 29° releasing fault bend marking the northern limit of the central Calaveras Fault. Several workers (WGCEP, 1999; Kelson, 2001) have proposed that this major change in strike is a segment boundary. Other north-striking fault traces occur near the Alum Rock epicenter (Plate 1a); along the northwestern margin of Halls Valley (Plate 1b); at the southeastern margin of lower San Felipe Valley (Plate 2a); within a landslide complex east of Anderson Lake (Plate 2a); and bounding the northwestern margin of a pull-apart basin at Coyote Lake (Plate 2b). In a regional sense, the overall pattern of north-trending fault traces that define the central Calaveras Fault exhibits a left-stepping en echelon organization and notably lacks a laterally continuous, narrow, well-defined fault trace. Such complexities may reflect relatively young deformation along the central Calaveras Fault zone and/or the heterogeneous bedrock geology in the Diablo Range.

The geometric complexity expressed at the surface is generally not reflected in patterns of microseismicity along the central Calaveras Fault (Figure 3). Several seismological studies have noted an apparent 2 km mismatch between the surface projection of microseismicity and the surface trace of the fault (Cockerham and Eaton, 1987; Oppenheimer et al., 1988). Relocated microseismicity data between the epicentral locations of the 1979 and 1988 earthquakes, using waveform cross correlation and double difference techniques, do not reduce the apparent eastward shift between the surface fault trace and seismicity at depths of 2 to 10 km (Schaff et al., 2002). However, several gross patterns recognized in the microseismicity data may be reflected at the surface. Microseismicity relocated by Schaff et al. (2002) shows a clear left-restraining stepover east of the southern end of Anderson Lake (Figure 3). This stepover, that may have influenced the rupture behavior of the 1984 Morgan Hill event, is reflected at the

surface as a left-restraining double bend along Coyote Creek between Coyote Dam and Anderson Lake (Plate 2a). Cockerham and Eaton (1987) noted that the surface trace of the fault between southern San Felipe Valley and the northwestern end of Anderson Lake reflects an alignment of diffuse 1984 aftershocks 7- to 8-km deep that are offset 2km southwest of a more prominent linear trend of seismicity. Finally, near the northern end of San Felipe Valley, the prominent linear alignment of relocated microseismicity takes a small step right that is possibly reflected by surficial fault traces that delineate 1.5- to 2-km wide pull-apart basin (Figure 3).

In the context of historic M >5 earthquakes, the surficial expression of active fault traces appears to reflect discrete subsegments of the central Calaveras Fault. Although the surface projection of microseismicity does not match the mapped surface trace, the rupture behaviors of the 1949, 1979, 1984, and 1988 earthquakes suggest that bends and stepovers defined by surficial fault traces reflect geometric or rheological rupture barriers along the fault in the subsurface. The lack of conclusive evidence for surface fault rupture during historic M >5 earthquakes, along with historic creep rates that approach estimates of the geologic slip rate, and the complex expression of the surface fault trace suggest that the current mode of failure involves rupture of 2.5- to 26-km-long fault subsegments. However, these observations do not preclude the possibility that future earthquakes may break multiple subsegments of the fault.

7.0 ACKNOWLEDGMENTS

This project was funded by the U.S. Geological Survey's National Earthquake Hazards Reduction Program (Award # 01HQGR0212). We would like to acknowledge W. Bryant and P. Wong of the California Geological Survey for providing digital copies of Fault Evaluation Reports and Alquist-Priolo geotechnical reports. J. Nelson of the Santa Clara Valley Water District provided preliminary GPS data and related information on the alignment arrays across Coyote Dam. Discussion with C. Wentworth improved the map.

8.0 REFERENCES

Andrews, D.J., Oppenheimer, D.H., and Lienkaemper, J.J., 1993, The Mission link between the Hayward and Calaveras Faults: Journal of Geophysical Research, v. 98, p. 12,083-12,095.

Armstrong, C.F., 1979, Coyote Lake earthquake 6 August 1979: California Geology, v. 32, p. 248-251.

Armstrong, C.F., and Wagner, D.L., 1978, Environmental geologic analysis of the Diablo Range Study Area, southern Santa Clara County, California: California Division of Mines and Geology Open-file Report OFR 78-11SF, scale 1:12,000.

Armstrong, C.F., Wagner, D.L., and Bortugno, E.J., 1980, Movement along the southern Calaveras Fault zone as shown by fence line surveys: Calif. Div. Mines and Geol. Spec. Rpt. 140, p. 29-39.

Atwater, B.F., 1982, Geologic maps of the Sacramento-San Joaquin Delta, California: U.S. Geological Survey Miscellaneous Field Studies Map MF-1401.

Atwater, B.F., Hedel, C.W., and Helley, E.J., 1977, Late Quaternary depositional history, Holocene sea-level changes, and vertical crustal movement, southern San Francisco Bay, California: U.S. Geological Survey Professional Paper 1014, 15 p.

Aydin, A. 1982, The East Bay hills, a compressional domain resulting from interaction between the Calaveras and Hayward-Rodgers Creek Faults, in Hart, E.W., Hirschfeld, S.E., and Schulz, S.S., eds., Proceedings of the Conference on Earthquake Hazards in the Eastern San Francisco Bay Area, California Division of Mines and Geology Special Publication 62, p. 11-21.

Aydin, A., and Page, B.M., 1984, Diverse Pliocene-Quaternary tectonics in a transform environment, San Francisco Bay region, California: Geological Society of America Bulletin, v. 95, p. 1303-1317.

Aydin, A. and Nur, A., 1985, The types and roles of stepovers in strike-slip tectonics, in Biddle, K.T. and Christie-Blick, N., eds., Strike-slip deformation, basin formation and sedimentation: SEPM Special Publication 37, p. 35-45.

Bakun, W.H., 1980, Seismic activity on the southern Calaveras Fault in central California: Bulletin of Seismological Society of America, v. 70, p. 1181-1197.

Bakun, W.H., Clark, M.M., Cockerham, R.S., Ellsworth, W.L., Lindh, A.G., Prescott, W.H., Shakal, A.F., and Spudich, P., 1984, The 1984 Morgan Hill, California, earthquake: Science, v. 225, p. 288-291.

Bakun, W.H. and Lindh, A.G., 1985, Potential for future damaging shocks on the Calaveras Fault, California: U.S. Geological Survey Open-file Report 85-754, p. 266-279.

Baldwin, J.N., Kelson, K.I., Witter, R.C., Koehler, R.D., Helms, J.G., and Barron, A.D., 2002, Preliminary report on the late Holocene slip rate along the central Calaveras Fault, southern San Francisco Bay area, Gilroy, California: Final Technical Report submitted to the National Earthquake Hazard Reduction Program, 27 p.

Barka, A.A. and Kadinsky-Cade, K., 1988, Strike-slip fault geometry in Turkey and its influence on earthquake activity: Tectonics, v. 7, p. 663-684.

Beroza, G.C., and Spudich, P., 1988, Linearized inversion for fault rupture behavior; application to the 1984 Morgan Hill, California, earthquake: Journal of Geophysical Research, v. 93, p. 6275-6296.

Bolt, B.A. and Miller, R.D., 1975, Catalogue of earthquakes in northern California and adjoining areas, in Seismographic Stations, University of California Press, Berkeley, p. 7-18.

Brown, B.D., 1987, Alignment Array Measurements in the San Felipe Valley, California: in, Hoose, S.A., (ed), The Morgan Hill, California, Earthquake of April 24, 1984, U.S. Geological Survey Bulletin 1639, p. 117-119.

Bryant, B. 1981a, Calaveras and Busch Ranch Faults, San Felipe quadrangle, San Benito and Santa Clara Counties: California Division of Mines and Geology Fault Evaluation Report 114.

Bryant, B. 1981b, Calaveras and related faults, La Costa Valley, Calaveras Reservoir, San Jose East, Mount Day, and Lick Observatory quadrangles, Alameda and Santa Clara Counties: California Division of Mines and Geology Fault Evaluation Report 115.

Bryant, B. 1981c, Calaveras, Coyote Creek, Animas, San Felipe, and Silver Creek Faults, Morgan Hill and Mt. Sizer quadrangles, southern Santa Clara County: California Division of Mines and Geology Fault Evaluation Report 122.

Campagna, D.J., and Aydin, A, 1991, Tertiary uplift and shortening in the Basin and Range: the Echo Hills, southeastern Nevada: Geology, v. 19, p. 485-488.

Chuang, F.C., Jachens, R.C., Wentworth, C.M., and Sanger, E.A., 2002, Young strike-slip basin on the Calaveras Fault in San Felipe Valley, California [abs]: Geological Society of America Abstracts with Program, v. 34, p. 99.

Cockerham, R.S., and Eaton, J.P., 1987, The earthquake and its aftershocks, April 24 through September 30, 1984: in, Hoose, S.A., (ed), The Morgan Hill, California, Earthquake of April 24, 1984, U.S. Geological Survey Bulletin 1639, p. 15-28.

Connelly, Steven F., 2002, Engineering geologic investigation, proposed 2-lot subdivision, APN 898-34-01, Leavesley Road, Santa Clara County, California, unpublished Alquist-Priolo report, AP#898-34-01, on file at the California Geological Survey, San Francisco, California, 38 p.

Cotton, W.R., 1972, Preliminary geologic map of the Franciscan rocks in the central part of the Diablo Range, Santa Clara and Alameda Counties, California: U.S. Geological Survey Misc. Invest. Map I-343, scale 1:62,500.

Cotton, W.R., Hall, N.T., and Hay, E.A., 1979, Preliminary field notes of the ground surface effects associated with the August 6, 1979, Coyote Lake earthquake: Consultants report prepared by William Cotton and Associates, 10 p.

Cotton, W.R., Hall, N.T., and Hay, E.A., 1986, Holocene behavior of the Hayward-Calaveras Fault system, San Francisco Bay area, California: Final Technical Report submitted to the National Earthquake Hazard Reduction Program, Award #14-08-0001-20555, U.S. Geological Survey, 26 p.

Crittenden, M.D., 1951, Geology of the San Jose - Mt. Hamilton area, California: California State Division of Mines Bulletin 157, 74 p.

Dibblee, T.W., Jr., 1972a, Preliminary geologic map of the Lick Observatory quadrangle, Santa Clara County, California: U.S., Geological Survey Open-file Report, scale 1:24,000.

Dibblee, T.W., Jr., 1972b, Preliminary geologic map of the San Jose East quadrangle, Santa Clara County, California: U.S., Geological Survey Open-file Report, scale 1:24,000.

Dibblee, T.W., Jr., 1973a, Preliminary geologic map of the Calaveras Reservoir quadrangle, Santa Clara County, California: U.S., Geological Survey Open-file Report 73-58, scale 1:24,000.

Dibblee, T.W., Jr., 1973b, Preliminary geologic map of the Gilroy 7-1/2' quadrangle, Santa Clara County, California: U.S., Geological Survey Open-file Map, scale 1:24,000.

Dibblee, T.W., Jr., 1973c, Preliminary geologic map of the Gilroy Hot Springs 7-1/2' quadrangle, Santa Clara County, California: U.S., Geological Survey Open-file Map, scale 1:24,000.

Dibblee, T.W., Jr., 1973d, Preliminary geologic map of the Morgan Hill quadrangle, Santa Clara County, California: U.S., Geological Survey Open-file Map, scale 1:24,000.

Dibblee, T.W., Jr., 1973e, Preliminary geologic map of the Mount Sizer 7-1/2' quadrangle, Santa Clara County, California: U.S., Geological Survey Open-file Map, scale 1:24,000.

Dibblee, T.W., Jr., 1975, Geologic map of the Hollister, Gonzales, and San Benito quadrangles: U.S. Geological survey Open-file Map 75-394, scale 1:62,500.

Du, Y. and Aydin, A., 1993, Stress transfer during three sequential moderate earthquakes along the central Calaveras Fault, California: Journal of Geophysical Research, v. 98, p. 9947-9962.

EMCON Associates, 1992, Report of disposal site information, Pacheco Pass Class III and Inert Waste Landfill, Santa Clara County, California, unpublished consulting report prepared for South Valley Refuse Disposal, Inc.

Geomatrix Consultants, 1994, Evaluation of landslide potential at the left abutment of Coyote Dam, unpublished final report prepared for Santa Clara Valley Water District, 68 p.

Graymer, R.W., 1997, Geology of the southernmost part of Santa Clara County, California: a digital database: U.S. Geological Survey Open-file Report 97-710.

Harms, K.K., Clark, M.M., Rymer, M.J., Bonilla, M.G., Harp, E.L., Herd, D.G., Lajoie, K.R., Lienkaemper, J.J., Mathieson, S.A., Perkins, J.A., Wallace, R. E., and Ziony, J.I., 1987, The search for surface faulting: in, Hoose, S.A., (ed), The Morgan Hill, California, Earthquake of April 24, 1984, U.S. Geological Survey Bulletin 1639, p. 61-68.

Harden, D.R., and Gallego, A., 1992, Recent disruption of Packwood Creek by the Calaveras Fault: in Borchardt, G., et al. (eds.), California Division of Mines and Geology Special Publication 113, p. 299-304.

Hart, E.W., 1984, Surface faulting associated with the Morgan Hill earthquake of April 24, 1984: California Geology, Santa Clara County, v. 37, p. 168-170.

Hart, E.W., Bryant, W.A., and Bedrossian, T.L., 1979, Observations of fault rupture associated with the August 6, 1979, earthquake and tabulation of observed data: California Division of Mines and Geology, in-house memo to C.F. Armstrong.

Hart, E.W., and Bryant, W.A., 1997, Fault-rupture hazard zones in California, California Division of Mines and Geology, Special Publication 42, 10th revision (with Supplements 1 and 2), pp. 47.

Helley, E.J., and Graymer, R.W., 1997, Quaternary geology of Alameda County, and parts of Contra Costa, Santa Clara, San Mateo, San Francisco, and San Joaquin Counties, California; a digital database: U.S. Geological Survey Open-file Report 97-0097.

Helley, E.J., Lajoie, K.R., Spangle, W.E., and Blair, M.L., 1979, Flatland deposits of the San Francisco Bay Region, California - Their geology and engineering properties, and their importance to comprehensive planning: U.S. Geological Survey Professional Paper 943, 88 p.

JCP—Engineers & Geologists, Inc., 1987, Engineering geologic and soil & foundation study for proposed residence on Felter Road, Santa Clara County, California, unpublished consulting report on file at the California Geological Survey, San Francisco, (AP #2710) 31 p.

Kelson, K.I., 2001, Geologic characterization of the Calaveras Fault as a potential seismic source, San Francisco Bay area, California, in Ferriz, H. and Anderson, R. (eds), Engineering Geology Practice in Northern California, Division of Mines and Geology Bulletin 210, Association of Engineering Geologists Special Publication 12, p. 179-192.

Kelson, K.I., Baldwin, J.N., and Brankman, C.M., 2003, Late Holocene displacement of the Central Calaveras Fault, Furtado Ranch Site, Gilroy, CA: Final Technical Report submitted to the National Earthquake Hazard Reduction Program, 38 p.

Kelson, K.I., Baldwin, J.N., and Randolph, C.E., 1998, Late Holocene slip rate and amounts of coseismic rupture along the central Calaveras Fault, San Francisco Bay area, California: Final Technical Report submitted to the National Earthquake Hazard Reduction Program, 26 p.

Kelson, K.I., Simpson, G.D., Lettis, W.R., and Haraden, C., 1996, Holocene slip rate and earthquake recurrence of the northern Calaveras Fault at Leyden Creek, northern California; Journal of Geophysical Research, v. 101, no. B3, p. 5961-5975.

Kelson, K.I., Lettis, W.R., and Lisowski, M., 1992, Distribution of geologic slip and creep along faults in the San Francisco Bay region: in Proceedings of the Second Conference on Earthquake Hazards in the Eastern San Francisco Bay Area, Borchardt, G. et al., (eds), California Division of Mines and Geology Special Publication 113, p. 31-38.

King, G.C.P., and Nábêlek, J.L., 1985, The role of bends in faults in the initiation and termination of earthquake rupture, Science, 228, 984-987.

Knudsen, K.L., Sowers, J.M., Witter, R.C., Wentworth, C.M., and Helley, E.J., 2000, Preliminary maps of Quaternary deposits and liquefaction susceptibility, nine-county San Francisco Bay region, California; a digital database: U.S. Geological Survey Open-File Report 00-444.

Lettis, W., J. Bachhuber, R. Witter, C. Brankman, C.E. Randolph, A. Barka, W.D. Page, and A. Kaya, 2002, Influence of releasing step-overs on surface fault rupture and fault segmentation: Examples from the 17 August 1999 Izmit earthquake on the north Anatolian Fault, Turkey, Bulletin of the Seismological Society of America, 92, 1, 19-42.

Lienkaemper, J.J., 1992, Map of recently active traces of the Hayward Fault, Alameda and Contra Costa Counties, California: U.S. Geological Survey Miscellaneous Field Studies Map MF-2196, map scale 1:24,000, 13 p.

Lienkaemper, J.J., Borchardt, G., and Lisowski, M., 1991, Historic creep rate and potential for seismic slip along the Hayward Fault, California, Journal of Geophysical Research, v. 96, p. 18,261-18,283.

Marliave, C., 1936, Final geologic report on Coyote Dam situated on Coyote River in Santa Clara County, California: Internal Report, State of California Department of Public Works, Division of Water Resources, 56 p.

Mathieson, S.A., 1987, Structural damage near Morgan Hill: in Hoose, S.A., (ed), The Morgan Hill, California, Earthquake of April 24, 1984, U.S. Geological Survey Bulletin 1639, p. 93-104.

Nakata, J.K., 1980, Distribution and petrology of the Anderson-Coyote Reservoir volcanic rocks, California: U.S. Geological Survey Open-File Report 80-1256.

Nilsen, T.H., Bartow, J.A., Frizzell, V.A., and Sims, J.D., 1975, Preliminary photointerpretation maps of landslide and other surficial deposits of 56 7.5-minute quadrangles in the southeastern San Francisco Bay region, Alameda, Contra Costa, and Santa Clara Counties, California: U.S. Geological Survey Open-file Report 75-277.

Oppenheimer, D.H., Bakun, W.H., and Lindh, A.G., 1990, Slip partitioning of the Calaveras Fault, CA, and prospects of future earthquakes: Journal of Geophysical. Research, v. 95, no. B6, p. 8483-8498. Oppenheimer, D.H., Reasenberg, P.A., and Simpson, R.W., 1988, Fault plane solutions for the 1984 Morgan Hill, California, earthquake sequence: Evidence for the state of stress on the Calaveras fault: Journal of Geophysical Research, v. 93, p. 9007-9026.

Page, B.M., 1982, The Calaveras Fault zone of California, an active plate boundary element, in Hart, E.W., Hirschfeld, S.E., and Schulz, S.S., eds., Proceedings of the Conference on Earthquake Hazards in the Eastern San Francisco Bay Area, California Division of Mines and Geology Special Publication 62, p. 175-184.

Page, B.M., Thompson, G.A. and Coleman, R.G., 1998, Late Cenozoic tectonics of the central and southern Coast Ranges of California, Geological Society of America Bulletin, v. 110, no. 7, p. 846-876.

Pampeyan, E.H., 1979, Preliminary map showing recency of faulting in coastal north-central California: U.S. Geological Survey Miscellaneous Field Studies Map MF-1070.

Radbruch-Hall, D.H., 1974, Map showing recently active breaks along the Hayward fault zone and the southern Calaveras fault zone, California: U.S. Geological Survey Misc. Investigations Series Map I-813, scale 1:24,000.

Rogers, T.H., 1973, Preliminary geologic map of the Hollister and San Felipe quadrangles: California Division of Mines and Geology, unpublished map, scale 1:24,000.

Rogers, T.H. and Nason, R.D., 1971, Active displacement on the Calaveras fault zone at Hollister, California: bulletin of the Seismological Society of America, v. 61, no. 2, p. 399-416.

Schaff, D.P, Bokelmann, G.H.R., Beroza, G.C., Waldhauser, F. and Ellsworth, W.L., 2002, High-resolution image of Calaveras Fault seismicity: Journal of Geophysical Research, v. 107, n. B9, ESE 5, p. 1-16.

Sieh, K., and Jahns, R., 1984, Holocene activity of the San Andreas Fault at Wallace Creek, California: Geological Society of America Bulletin, v. 95, p. 883-896.

Sharp, R. V., 1972, Map showing recently active breaks along the San Jacinto Fault zone between the San Bernardino area and the Borrego Valley, California, Miscellaneous Geologic Investigations Map, I-0675, scale 1:24,000.

Simpson, G.D. and Lettis, W.R., 1992, Segmentation model for the northern Calaveras Fault, Sunol Valley to Walnut Creek: in Proceedings of the Second Conference on Earthquake Hazards in the Eastern San Francisco Bay Area, Borchardt, G. et al., (eds), California Division of Mines and Geology Special Publication 113, p. 240-246.

Simpson, G.D., Baldwin, J.N., Kelson, K.I., and Lettis, W.R., 1999, Late Holocene slip rate and earthquake history for the northern Calaveras Fault at Welch Creek, eastern San Francisco Bay area, California: Bulletin of the Seismological Society of America, v. 89, no. 5, p. 1250-1263.

Smith, T.C., 1981, Calaveras and related faults, Gilroy and Gilroy Hot Springs quadrangles, southern Santa Clara County, California: California Division of Mines and Geology Fault Evaluation Report 121.

Toppozada, T.R. and Parke, D.L., 1982, Areas damaged by California earthquakes, 1900-1949, Open File Report 82-17 SAC, California Division of Mines and Geology, Sacramento, 65 pp.

Toppozada, T.R., Real, C.R., and Parke, D.L., 1981, Preparation of isoseismal maps and summaries of reported effects for pre-1900 California earthquakes, Open File Report 81-11 SAC, California Division of Mines and Geology, Sacramento, 182 pp.

Unruh, J.R. and Lettis, W.R., 1998, Seismogenic deformation field in the Mojave block and implications for tectonics of the eastern California shear zone: Journal of Geophysical Research, v. 101, p. 8335-8361.

U.S. Department of Agriculture, 1939, Stereographic, black and white, vertical aerial photography, Series CIV, Roll Nos.284, 294, 299, Approximate scale: 1:20,000.

U.S. Department of Agriculture, 1940, Stereographic, black and white, vertical aerial photography, Series CIV, Roll No.R351, Approximate scale: 1:20,000.

WAC Corp., 1999, Stereographic, color, vertical aerial photography, Series WAC-C-99CA, Roll Nos. 6, 7, and 8, Approximate scale: 1:24,000.

WAC Corp. 2000, Stereographic, black and white, vertical aerial photography, WAC-00-CA, Roll Nos. 27 and 29, Approximate scale: 1:24,000.

Wagner, D.L., 1978, Environmental geologic analysis of the Diablo Range Study Area II, southern Santa Clara County, California: California Division of Mines and Geology Open-file Report 78-12, 46 p., 3 plates.

Wallace, R.E., 1990, The San Andreas Fault System, California: U.S. Geological Survey Professional Paper 1515, United States Government Printing Office, Washington, D. C., 283 p.

Wentworth, C.M., Blake, M.C., Jr., McLaughlin, R.J., and Graymer, R.W., 1999, Preliminary geologic map of the San Jose 30 X 60 minute quadrangle, California: U.S. Geological Survey Open-file Report 98-795.

Williams, J.W., Armstrong, C.F., Hart, E.W., and Rogers, T.H., 1973, Environmental geological analysis of the South County Study Area, Santa Clara County, California: California Division of Mines and Geology Preliminary Report 18.

Wong, I.G. and Hemphill-Haley, M.A., 1992, Seismicity and faulting near the Hayward and Mission Faults, in Proceedings of the Second Conference on Earthquake Hazards in the Eastern San Francisco Bay Area, Borchardt, G. et al., (eds), California Division of Mines and Geology Special Publication 113, p. 207-215.

WGCEP (Working Group on California Earthquake Probabilities), 1999, Earthquake probabilities in the San Francisco Bay region: 2000 to 2030--A summary of findings: U.S. Geological Survey Open-file Report 99-517.

APPENDIX A - DESCRIPTION OF GEOLOGIC UNITS

Map Symbol	Unit Name and Description
	MODERN (<150 YEARS) DEPOSITS
af	**Artificial fill (historical).** Engineered and/or non-engineered material deposited by humans; each may occur within the same area on the map. Mapping of artificial fill is based on inspection of topographic maps and aerial photographs. Most of the artificial fill shown consists of engineered fill up to approximately 200 feet thick used in the construction of large earthen dams. Fill less than 10- to 20-feet thick (less than the contour interval) and fill emplaced after the topographic base maps were surveyed are not shown. Small bodies of fill, such as small road embankments and earthen dams for farm ponds, are not shown.
ac	**Artificial stream channel (historical).** Modified stream channels including straightened or realigned channels, flood control channels, channels bordered by dikes or levees, and concrete canals. In most cases, artificial channels were differentiated from natural channels by interpretation of 7.5-minute topographic quadrangles. Additionally, field inspection and interpretation of aerial photographs were used to identify artificial channels. Deposits within artificial channels can range from nonexistent in some concrete canals, to loose, unconsolidated sand, gravel and cobbles, similar to deposits of modern stream channel deposits (Qhc).
Qhc	**Modern stream channel deposits.** Fluvial deposits within active, natural stream channels. Materials consist of loose, unconsolidated, poorly to well sorted sand, gravel and cobbles, with minor silt and clay. These deposits are reworked by frequent flooding and exhibit no soil development. These deposits fine downstream (i.e. sediment is coarser upstream). Mapping of modern stream channels is based on topographic map inspection augmented, in places, by interpretation of aerial photography. Contacts generally are shown near the top of the bank on either side of the channel, although the deposits actually lie near the bottom of the bank.
	LATEST HOLOCENE (<1,000 YEARS)
Qhfy	**Latest Holocene alluvial fan deposits.** Alluvial fan sediment judged to be latest Holocene (<1,000 years) in age, based on records of historical inundation or the presence of youthful braid bars and distributary channels. Youthfulness of braid bars and distributary channels was evaluated using aerial photographs. Alluvial fan sediment is deposited by streams emanating from mountain canyons onto alluvial valley floors or alluvial plains. A primary example of this is the Calaveras Creek fan at the southern end of Calaveras Reservoir. Sediment is moderately to poorly sorted

and bedded, and may be composed of gravel, sand, silt and clay. Grain size generally fines downslope.

Qhty **Latest Holocene stream terrace deposits.** Stream terrace deposits judged to be latest Holocene (<1,000 years) in age based on the identification of youthful meander scars and braid bars on aerial photographs s, and geomorphic position (elevation) very close to the stream channel. Stream terrace sediment includes sand, gravel, silt, and minor clay, is moderately to well sorted, and is moderately to well bedded.

Qhay **Latest Holocene alluvial deposits, undifferentiated.** Fluvial sediment judged to be latest Holocene (<1000 years) in age based on records of historical inundation, the identification of youthful meander scars and braid bars on aerial photographs, or geomorphic position very close in elevation to the stream channel. This sediment was deposited on modern flood plains, active stream channels, active alluvial fans, and flood-prone areas. Deposits are loose sand, gravel, silt and clay. This unit is mapped in areas that historically have been inundated by sediment-bearing water. Latest Holocene alluvial deposits may include terrace deposits (Qhty), deposits of the active stream channel (Qhc), alluvial fan deposits (Qhfy), and basin deposits (Qhb). However, the small size of individual deposits of these map units prevented differentiation at the map scales used in this project.

HOLOCENE (<10,000 YEARS)

Qhb **Holocene basin deposits.** Sediment that accumulates from standing or slow moving water in topographic basins. Basin deposits consist of fine-grained alluvium with horizontal stratification. These deposits can be interbedded with lobes of coarser alluvium from streams that drain into the basin. Interbeds of peat may also be present. Identification of basin deposits is based on surface morphology, topographic position, and soil type. Ground water is high, often at the surface, especially during the rainy season. Many basins occur in closed depressions or sag ponds created by local areas of extension or grabens along the Calaveras fault.

Qhf **Holocene alluvial fan deposits.** Sediment deposited by streams emanating from mountain canyons onto alluvial valley floors or alluvial plains as debris flows, hyperconcentrated mudflows, or braided stream flows. Alluvial fan sediment includes sand, gravel, silt, and clay, and is moderately to poorly sorted, and moderately to poorly bedded. Sediment clast size and general particle size typically decreases downslope from the fan apex. Alluvial fan surfaces are steepest near their apex at the valley mouth, and slope gently basinward, typically with gradually decreasing gradient. Alluvial fan deposits are identified primarily on the basis of fan morphology and topographic expression. Holocene alluvial fans are relatively undissected, especially when compared to older alluvial fans. In places, Holocene deposits may be only a thin veneer over Pleistocene deposits.

Qhl **Holocene alluvial fan levee deposits.** Natural levee deposits of alluvial fans are formed by streams that overtop their banks and deposit sediment adjacent to the

channel. Mapping of these deposits is based on interpretation of topography; levees are identified as long, low ridges oriented down fan ["channel ridges" of Thomasson et al. (1960)]. They contain coarser material than adjoining interlevee areas, especially adjacent to creek banks where the coarsest material is deposited during floods (Helley et al., 1979). Levee deposits are loose, moderately to well sorted sand, silt and clay (Helley and Wesling, 1989).

Qhff **Holocene alluvial fan deposits, fine facies.** Fine-grained alluvial fan and flood plain overbank deposits laid down in very gently sloping portions of the alluvial fan or valley floor. Slopes in these distal alluvial fan areas are generally less than or equal to 0.5 degrees, soils are clay rich, and ground water is within 3 meters of the surface. Deposits are dominated by clay and silt, with interbedded lobes of coarser alluvium (sand and occasional gravel). Deposits of coarse material within these fine-grained materials are elongated in the downfan or down valley direction. These lobes are potential conduits for ground water flow. The surface contact with relatively coarser facies, fan (Qhf) and levee (Qhl), is both gradational and interfingering, thus is dashed.

Qht **Holocene stream terrace deposits.** Stream terrace deposits that were deposited in point bar and overbank settings. Terrace deposits include sand, gravel, silt, and minor clay, and are moderately to well sorted, and moderately to well bedded. This unit is mapped where relatively smooth, undissected terraces are less than 25 to 30 ft above the active channel. Ground-water levels are generally within 10 ft of the surface, especially during the wet winter months. Terrace deposits that are too small in extent to be shown at the map scale, such as those along small creeks, are included within the undifferentiated alluvium (Qha and Qa) mapping units.

Qha **Holocene alluvium, undifferentiated.** Alluvium deposited in fan, terrace, or basin environments. This unit is mapped where separate types of alluvial deposits could not be delineated either due to complex interfingering of depositional environments or the small size of the area. Undifferentiated alluvium is mapped in relatively flat, smooth valley bottoms of small- to medium-sized drainages. The planar and smooth geomorphic surfaces, with little to no dissection, indicate that there has been little post-stabilization modification/dissection of the surface; thus, deposits with smooth surfaces are interpreted to be Holocene in age. Undifferentiated Holocene alluvial deposits probably are intercalated sand, silt, and gravel that are poorly to moderately sorted.

HOLOCENE TO LATE PLEISTOCENE (<30,000 YEARS)

Qb **Late Pleistocene to Holocene basin deposits.** Sediment deposited in topographic lows, such as a closed or semi-enclosed basin. These areas have a high ground-water table and poorly drained soils. Deposits are generally clay rich.

Qf **Late Pleistocene to Holocene alluvial fan deposits.** This unit is mapped on gently sloping, fan-shaped, relatively undissected alluvial surfaces where the age of deposits

(either late Pleistocene or Holocene in age) or where the deposits consist of thin "patches" of Holocene sediment overlying late Pleistocene alluvial fan sediment. Fan sediment includes sand, gravel, silt, and clay, and is moderately to poorly sorted, and moderately to poorly bedded.

Qa **Late Pleistocene to Holocene alluvium, undifferentiated.** This unit is mapped in small valleys where separate fan, basin, and terrace units could not be delineated at the scale of this mapping, and where deposits might be of either late Pleistocene or Holocene age. The unit includes flat, relatively undissected fan, terrace, and basin deposits, and small active stream channels.

LATE PLEISTOCENE (11,000 to 125,000 YEARS)

Qpf **Late Pleistocene alluvial fan deposits.** This unit is mapped on alluvial fans where late Pleistocene age is indicated by greater dissection than is present on Holocene fans, and/or the development of alfisols. Late Pleistocene alluvial fan sediment was deposited by streams emanating from mountain canyons onto alluvial valley floors or alluvial plains as debris flows, hyperconcentrated mudflows, or braided stream flows. Alluvial fan sediment typically includes sand, gravel, silt, and clay, and is moderately to poorly sorted, and moderately to poorly bedded. Sediment clast size and general particle size typically decreases downslope from the fan apex. Pleistocene alluvial fans may be veneered or incised by thin unmapped Holocene alluvial fan deposits.

Qpt **Late Pleistocene stream terrace deposits.** This unit is mapped on relatively flat, slightly dissected stream terraces where late Pleistocene age is indicated by the development of alfisols and height of the terrace above flood level. Terrace sediment includes sand, gravel, silt, with minor clay, and is moderately to well sorted, and moderately to well bedded. Terrace sediment typically was deposited in point bar and overbank settings and has since been elevated above the creek bottom by incision of the streambed. Late Pleistocene terrace deposits that are too small in extent to be shown at the map scale, such as those along small creeks, may be included within the undifferentiated late Pleistocene and late Pleistocene to Holocene alluvial mapping units (Qpa and Qa).

Qpa **Late Pleistocene alluvium, undifferentiated.** This unit is mapped on gently sloping to level alluvial fan or terrace surfaces where late Pleistocene age is indicated by depth of stream incision, and lack of historical flooding. Undifferentiated late Pleistocene alluvium is mapped in small valleys where separate fan, basin, and terrace units could not be delineated at the mapping scale of this project. These undifferentiated late Pleistocene alluvial deposits probably are intercalated sand, silt, and gravel that are poorly to moderately sorted.

EARLY TO MIDDLE PLEISTOCENE (>125,000 to 2MYRS)

Qof **Early to middle Pleistocene alluvial fan deposits.** Moderately to deeply dissected alluvium deposited by streams emanating from mountain canyons onto alluvial valley floors or alluvial plains as debris flows, hyperconcentrated mudflows, or braided stream flows. Because of the age of these deposits, the streams responsible for deposition of mapped bodies of early to middle Pleistocene alluvial fan sediment may have evolved and no longer be readily evident in today's topography. Alluvial fan sediment typically includes sand, gravel, silt, and clay, and is moderately to poorly sorted, and moderately to poorly bedded. This unit differs from undifferentiated early to middle alluvium (Qoa) in that some original fan surface morphology is preserved.

Qot **Early to Middle Pleistocene stream terrace deposits.** Moderately to deeply dissected alluvial terrace deposits consisting of sand, gravel, and silt, with minor clay, that is moderately to well sorted, and moderately to well bedded. Terrace sediment typically was deposited in point bar and overbank settings and has since been elevated above the creek bottom by incision of the streambed. This unit differs from Qoa in that some terrace surface morphology is preserved.

Qoa **Early to middle Pleistocene alluvial deposits, undifferentiated.** Moderately to deeply dissected alluvial deposits. Topography often consists of gently rolling hills with little or none of the original planar alluvial surface preserved. Deposits mapped within this map unit can include alluvial fan, stream terrace, basin and channel deposits.

br **Pre-Quaternary deposits and bedrock, undifferentiated.** Primarily Jurassic and Cretaceous sedimentary, metamorphic and igneous rocks of the Coast Range Ophiolite, Franciscan Complex, and Berryessa Formation. Overlying Neogene sedimentary rocks include the Middle Miocene Temblor Sandstone, the Middle to Upper Miocene Claremont and Briones Formations, and Plio-Pleistocene Silver Creek and Packwood gravels. Unit also includes small landslides, talus, other bodies of colluvium, and small stream channel deposits in bedrock that could not be delineated at the map scales used in this project.

ABBREVIATED REFERENCE CODES

AP898-34-01— Connelly, Steven F., 2002, Engineering geologic investigation, proposed 2-lot subdivision, APN 898-34-01, Leavesley Road, Santa Clara County, California, unpublished Alquist-Priolo report, AP#898-34-01, on file at the California Geological Survey, San Francisco, California.

AP1165—Terratech Technical Services, Inc., 1980, Combined geologic and geotechnical investigation, Edelweiss Ranch—Lands of Vogt, Santa Clara County, California, unpublished consulting report on file at the California Geological Survey, San Francisco, (AP #1165) 50 p.

AP2710—JCP—Engineers & Geologists, Inc., 1987, Engineering geologic and soil & foundation study for proposed residence on Felter Road, Santa Clara County, California, unpublished consulting report on file at the California Geological Survey, San Francisco, (AP #2710) 31 p.

B02—Baldwin, J.N., Kelson, K.I., Witter, R.C., Koehler, R.D., Helms, J.G., and Barron, A.D., 2002, Preliminary report on the late Holocene slip rate along the central Calaveras Fault, southern San Francisco Bay area, Gilroy, California: Final Technical Report submitted to the National Earthquake Hazard Reduction Program, 27 p.

C86—Cotton, W.R., Hall, N.T., and Hay, E.A., 1986, Holocene behavior of the Hayward-Calaveras Fault system, San Francisco Bay area, California: Final Technical Report submitted to the National Earthquake Hazard Reduction Program, Award #14-08-0001-20555, U.S. Geological Survey, 26 p.

G94—Geomatrix Consultants, 1994, Evaluation of landslide potential at the left abutment of Coyote Dam, unpublished final report prepared for Santa Clara Valley Water District, 68 p.

K03—Kelson, K.I., Baldwin, J.N., and Brankman, C.M., 2003, Late Holocene displacement of the Central Calaveras Fault, Furtado Ranch Site, Gilroy, CA: Final Technical Report submitted to the National Earthquake Hazard Reduction Program, 38 p.

M36—Marliave, C., 1936, Final geologic report on Coyote Dam situated on Coyote River in Santa Clara County, California: Internal Report, State of California Department of Public Works, Division of Water Resources, 56 p.